

**Technical Report 1693**  
February 1995

# **WWVB Antenna and Antenna Tuning System**

Baseline Measurements

Peder M. Hansen  
NCCOSC RDT&E Division

Darrell Gish  
Pacific Sierra Research Corporation



**Technical Report 1693**

February 1995

# **WWVB Antenna and Antenna Tuning System**

Baseline Measurements

Peder M. Hansen  
NCCOSC RDT&E Division

Darrell Gish  
Pacific Sierra Research Corporation

**NAVAL COMMAND, CONTROL AND  
OCEAN SURVEILLANCE CENTER  
RDT&E DIVISION  
San Diego, California 92152-5001**

---

---

**K. E. EVANS, CAPT, USN**  
Commanding Officer

**R. T. SHEARER**  
Executive Director

## **ADMINISTRATIVE INFORMATION**

The work described in this document was carried out by personnel from the Naval Command, Control and Ocean Surveillance Center, RDT&E Division (NRaD), and the Pacific Sierra Research Corporation. Sponsorship was provided by the Space and Naval Warfare Systems Command.

Released by  
P. A. Singer, Head  
Systems Development  
Branch

Under authority of  
B. M. Bauman, Head  
Submarine Communications  
Division

## **ACKNOWLEDGMENTS**

The authors wish to express appreciation for the exceptional efforts by the WWV site personnel, who offered extra time and energy and were very responsive in helping the on-site testing to be performed as efficiently and smoothly as possible.

## EXECUTIVE SUMMARY

The National Institute of Standards and Technology (NIST) operates a 60-kHz timing signal transmitter, known as WWVB, at a site near Fort Collins, Colorado. This system has redundant transmitters and antenna systems and was thought to radiate about 13 kW. NIST commissioned the Naval Command, Control and Ocean Surveillance Center, Research, Development, Test and Evaluation Division (NRaD) to make baseline performance measurements that could support the design of a 6-dB upgrade.

NRaD tasked the Pacific Sierra Research Corporation (PSR) to perform the baseline antenna and antenna tuning system measurements; NRaD performed the antenna effective height measurements. The measurements were made from 10 October to 20 October 1994. This document presents these measurements. A second document, NRaD TR 1692, provides a summary of the measurement results, a recommended upgrade configuration, and recommendations.



# CONTENTS

<b>1. INTRODUCTION</b> .....	<b>1</b>
1.1 BACKGROUND .....	1
1.2 SUMMARY .....	2
<b>2. ANTENNA AND ANTENNA TUNING SYSTEM MEASUREMENTS</b> .....	<b>4</b>
2.1 MEASUREMENT METHOD .....	4
2.2 GROSS RESISTANCE AND ANTENNA SYSTEM BANDWIDTH .....	4
2.3 ANTENNA PARAMETERS .....	4
2.3.1 Antenna Capacitance .....	13
2.3.2 Antenna Base Reactance .....	13
2.3.3 Antenna Resonance .....	13
2.3.4 Antenna Downlead Inductance .....	13
2.4 ANTENNA TUNING HELIX .....	14
2.5 ANTENNA TUNING VARIOMETER .....	16
2.6 ANTENNA TUNING SYSTEM RESISTANCE .....	16
2.7 MUTUAL IMPEDANCE BETWEEN ANTENNAS .....	16
2.8 TRANSMISSION LINES .....	21
2.9 ANTENNA AND TUNING SYSTEM CIRCUIT MODEL .....	23
2.10 GROUND CONDUCTIVITY MEASUREMENTS .....	27
<b>3. EFFECTIVE HEIGHT MEASUREMENTS</b> .....	<b>29</b>
3.1 BACKGROUND .....	29
3.2 CURRENT MONITOR LOCATION .....	29
3.3 MEASUREMENTS .....	29
3.3.1 Antenna Current Measurements .....	31
3.3.2 Navigation .....	31
3.3.3 Magnetic Field Measurement .....	32
3.4 MEASUREMENT RESULTS .....	33
3.5 DISCUSSION .....	34
<b>4. OTHER MEASUREMENTS</b> .....	<b>36</b>
4.1 GENERAL .....	36
4.2 LITZ WIRE .....	36
4.3 GROUND SYSTEM .....	37
4.4 NEAR-FIELD MEASUREMENTS UNDER TOPLOAD .....	38
<b>5. REFERENCES</b> .....	<b>39</b>

## Appendices

<b>APPENDIX A: RAW BASELINE IMPEDANCE DATA .....</b>	<b>A-1</b>
<b>APPENDIX B: PHYSICAL MEASUREMENTS .....</b>	<b>B-1</b>
<b>APPENDIX C: WWVB ANTENNA CURRENT METER CALIBRATION .....</b>	<b>C-1</b>
<b>APPENDIX D: HELMHOLTZ COIL CALIBRATION .....</b>	<b>D-1</b>

## Figures

1. General setup for impedance measurements .....	4
2. WWVB primary antenna impedance .....	5
3. WWVB secondary antenna impedance .....	5
4. WWVB antenna circuit model (primary and secondary) .....	14
5. Helix circuit models .....	15
6. Helix house variometer inductance versus position .....	17
7. Linear two-port network model of two coupled antennas .....	18
8. Mutual impedance circuit model of antennas (60 kHz) .....	21
9. WWVB primary antenna and tuning system circuit model .....	24
10. WWVB secondary antenna and tuning system circuit model .....	25
11. WWVB mutual impedance circuit model .....	26
12. Average ground conductivity around WWVB .....	28
13. WWVB antenna effective height .....	34
C-1. Primary antenna current meter calibration .....	C-3
C-2. Secondary antenna current meter calibration .....	C-3
D-1. Helmholtz coil calibration setup .....	D-3
D-2. Helmholtz coil calibration, before measurements .....	D-4
D-3. Helmholtz coil calibration, after measurements .....	D-4
D-4. Blue loop calibration, before measurements .....	D-5
D-5. Blue loop calibration, after measurements .....	D-5

## Tables

1.	WWVB antenna and tuning system measurement summary .....	3
2.	WWVB primary antenna impedance data listing .....	6
3.	WWVB secondary antenna impedance data listing .....	10
4.	WWVB mutual impedance measurement data .....	21
5.	Transmission line parameters .....	22
6.	Average ground conductivity .....	28
7.	WWVB field strength measurement sites .....	30
8.	WWVB radiation efficiency (60-kHz operation) .....	35
A-1.	WWVB data disk log .....	A-2
C-1.	Antenna current meter calibration data .....	C-2



# 1. INTRODUCTION

## 1.1 BACKGROUND

The National Institute of Standards and Technology (NIST), formerly the National Bureau of Standards, provides services that broadcast accurate time and frequency signals. One of these services, known as WWVB, is a low-frequency (LF) broadcast on 60 kHz from their Fort Collins, Colorado, transmitting site. This service originally initiated from a site in Boulder in July 1956 and transmits time and frequency signals at 60 kHz, primarily for the continental United States. WWVB was moved to the site in Fort Collins in July 1963 and on 1 July 1965 began broadcasting the time information using a level-shift carrier time code. The code is binary-coded decimal (BCD), which is broadcast continuously, and the modulation is synchronized with the 60-kHz carrier signal (Beehler & Lombardi, 1991). The modulation is formed from full-power pulses with a duty cycle of approximately 50 percent. The signal between pulses is 10 dB below full power. The narrowest pulse is 0.2 second long, implying a system bandwidth requirement of approximately 5 Hz.

Originally, there was also an experimental very low-frequency (VLF) time signal on 20 kHz, known as WWVL, which was initiated in 1960 from a location at Sunset, Colorado. This station was moved to Fort Collins at the same time as WWVB (July 1963) but has since ceased operations.

Two antennas are used for the WWVB LF broadcast. The antenna feeds are located approximately 1500 feet away from the transmitter building in opposite directions. Each has its own helix house containing the tuning inductance, consisting of a fixed helix coil and a variometer (variable inductor). The antenna to the south was originally used for the 60-kHz broadcast and is still the primary antenna for that service. The antenna to the north was originally used for the 20-kHz broadcast and is now used as the backup antenna for the 60-kHz system.

The two transmitters that support this broadcast were built from surplus military HF transmitters (possibly FRT-6s). They are called “Old Blue” and “Old Grey” and are quite different in configuration. They were modified significantly from their original configuration, and very little documentation is available for these transmitters. The two transmitters are not identical but are said to be rated at 50 kW. The grey transmitter uses four 3CX10,000 tubes with an iron core transformer coupled output that appears to be set up to have a 500-ohm output impedance. The blue transmitter uses 12 2CX1,500 tubes and has a class C tuned output configuration for which the output impedance is unknown.

The original 60-kHz system (grey transmitter on south antenna) is the primary transmitting system. The backup, or secondary system, consists of the blue transmitter on the north antenna. Provisions have been made to enable switching the blue transmitter to operate on the south antenna as an additional backup mode.

The two antennas are identical with nearly identical helix houses. Documentation for the antenna systems is sparse. The antenna toploads are diamond-shaped panels supported by 400-foot towers with a center download. The panels have eight long wires running the long way of the diamond that form the main portion of the topload. These wires are supported in the center by a support cable that goes across the diamond. This diamond-shaped antenna is sometimes referred to as a triatic antenna. Each corner of the topload is counterweighted with a cable that runs down to the tower base. The antenna download feed uses a six-wire cage in a counterweighted dog-leg configuration. The down-

A balanced two-wire elevated transmission line is used to feed each helix house. In the helix house, the transmission line feeds a few turns on the helix as a transformer primary, which provides the impedance match between the “1 ohm” antenna and the transmission line. A separate winding is connected as the secondary that feeds the antenna. The secondary is connected to the antenna directly and to ground through a small variometer. The variometer is used to tune the antenna for environmental variations.

The system was designed and built by W.W. Brown around 1958. Since that time, there have been some modifications, including changes to the ground system. Based on some old data, at 60 kHz the antennas are thought to have 1-ohm total resistance and to be about 30 percent efficient. The radiated power, during pulse maximums, is thought to be about 13 kW.

NIST needs to upgrade the LF broadcast, with an objective of about a 6-dB increase in radiated power, or to about 50 kW radiated. This objective may be achieved by increasing efficiency and/or increasing transmitter power.

NIST tasked the Research, Development, Test and Evaluation Division of the Naval Command, Control and Ocean Surveillance Center (known as NRaD) to provide system measurements of the existing antenna and tuning and matching components. The measurements will baseline the existing system for analysis and engineering in support of the upgrade. NRaD tasked Pacific Sierra Research Corporation (PSR) to perform the baseline antenna and antenna tuning system measurements; NRaD performed the antenna effective height measurements.

## **1.2 SUMMARY**

The antenna and antenna tuning system were measured from 10 October to 20 October 1994. Darrell Gish of PSR and Dr. Peder Hansen and Jim Birkett of NRaD performed the measurements.

Table 1 lists critical quantities measured and summarizes the results for each antenna, primary (south) and secondary (north). Detailed descriptions of the measurements are presented in section 2. Schematic diagrams of the WWVB antenna and tuning system are included in section 2 that represent circuit models useful for system circuit analysis. Extended frequency measurements, to 1 MHz, were made of the antenna to facilitate system analysis of conducted harmonics, electromagnetic propagation (EMP), etc., and these frequency measurements are also presented in section 2. All raw data were stored on magnetic disk by an HP 4195A network analyzer. The data disk is catalogued in appendix A. Appendix B lists the results of physical measurements of the transmission line, antenna, and helix house components. Appendix C gives the results of current meter calibrations performed for the primary and secondary antenna current meters, and appendix D describes the Helmholtz calibration of the loop antenna used for the field strength measurements.

**Table 1.** WWVB antenna and tuning system measurement summary.

Parameter	Symbol	Measured Value		Section
		Primary	Secondary	
Gross Resistance	$R_g$	0.803 $\Omega$	0.913 $\Omega$	2.2
Antenna System Intrinsic Bandwidth	BW	263 Hz	310 Hz	2.2
Antenna Static Capacitance	$C_0$	14.7 nF	14.6 nF	2.3.1
Antenna Topload Capacitance	$C_t$	13.6 nF	13.6 nF	2.3.1
Antenna Base Stray Capacitance	$C_s$	1.1 nF	1.0 nF	2.3.1
Antenna Base Reactance @ 60.0 kHz	$X_b$	-114.9 $\Omega$	-112.9 $\Omega$	2.3.2
Antenna First Resonance	$f_0$	94.4 kHz	94.8 kHz	2.3.3
Antenna Downlead Inductance @ 60.0 kHz	$L_d$	208.8 $\mu$ H	208.0 $\mu$ H	2.3.4
Antenna Radiation Resistance	$R_r$	0.462 $\Omega$	0.462 $\Omega$	3.5
Antenna Effective Height	$h_e$	85.5 m	85.5 m	3.4
Antenna Loss Resistance	$R_{al}$	0.206 $\Omega$	0.321 $\Omega$	3.5
Antenna Radiation Efficiency	$\eta$	57.5%	50.6%	3.5
Helix Inductance	$L_H$	278.4 $\mu$ H	212.5 $\mu$ H	2.4
Tuning Variometer Inductance (typical)	$L_V$	26.4 $\mu$ H	87.0 $\mu$ H	2.5
Tuning System Loss Resistance @ 60.0 kHz	$R_t$	0.135 $\Omega$	0.130 $\Omega$	2.6
Antenna Mutual Impedance = Mutual Resistance + Mutual Reactance	$Z_m$	$Z_M = R_M + jX_M$ $= 0.377 - j0.652 \Omega$		2.7
Transmission Line Characteristic Impedance	$Z_0$	522 $\Omega$	535 $\Omega$	2.8
Transmission Line Electrical Length	$\phi_L$	31.31 $^\circ$	31.72 $^\circ$	2.8
Transmission Line Physical Length	$\ell$	1427 ft	1450 ft	2.8

## 2. ANTENNA AND ANTENNA TUNING SYSTEM MEASUREMENTS

This section describes the results of the baseline measurements on the WWVB antenna and antenna tuning system. The primary frequency of interest is 60.0 kHz, and the primary band of interest, the “in-band” region, is only approximately 5 Hz around 60.0 kHz. Due to the convenience and speed of the measurement technique used, most of the raw data consists of 401 frequencies within  $\pm 500$  Hz of 60.0 kHz. The breadth of the data provides a good overview of the in-band character of each measured quantity. Measurements of the antenna base impedance from 10 kHz to 1 MHz are called “out-of-band” data; these measurements are also presented in this section.

### 2.1 MEASUREMENT METHOD

Figure 1 shows the general test setup, which used a network analyzer to measure complex impedance. The device under test (DUT) could be a resistor, a capacitor, an inductor, an antenna, or any combination of these. The impedance probe shown in the figure is a custom module designed and built by PSR engineers to permit accurate complex impedance measurements of large components and subsystems located tens or hundreds of feet from the network analyzer. The antenna system impedance measurements used this method to measure complex impedance at the nodes described, from which inductance, capacitance, and resistance are derived. The network analyzer has an output that generates a sine wave, swept from a start frequency to a stop frequency. The two inputs to the analyzer have adaptive filters that are synchronized to the output frequency and are used to sample voltages (or currents) in the test circuit. The analyzer displays the inputs (or ratios of the inputs) and can perform math operations on the inputs prior to display. In this manner, the analyzer is used to measure the complex impedance of the item under test; the impedance can be displayed as magnitude and phase or as real and imaginary components. An external amplifier is used to increase the signal-to-noise ratio of the measured quantities; this is especially useful when measuring antenna impedances because the environment in which the antennas are placed is generally very noisy.

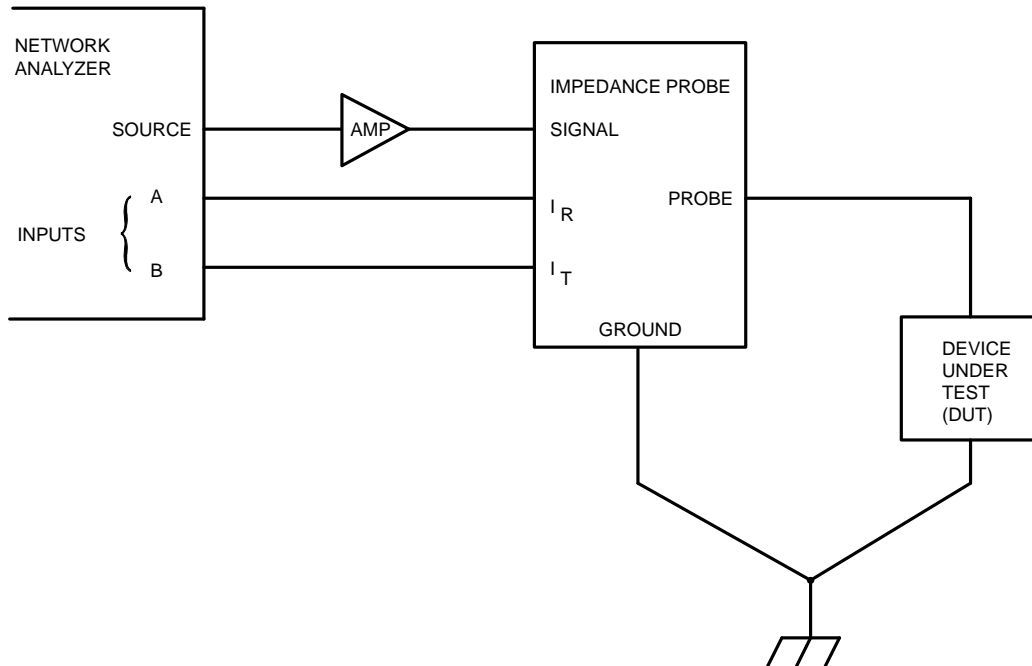


Figure 1. General setup for impedance measurements.

The network analyzer measurements produce data that may be plotted and/or listed in tabular format directly by the analyzer. In addition, all network analyzer raw data have been recorded on magnetic media and may be accessed for further analysis at any time in the future. However, the raw data is very bulky, and all of the pertinent data have been interpreted in this report to describe the baseline measurements of the WWVB antenna and tuning system. Therefore, printouts of the raw data, with the exception of the antenna base impedance, are excluded from this report. As a courtesy, the contents of the raw data on the data disk have been catalogued in appendix A.

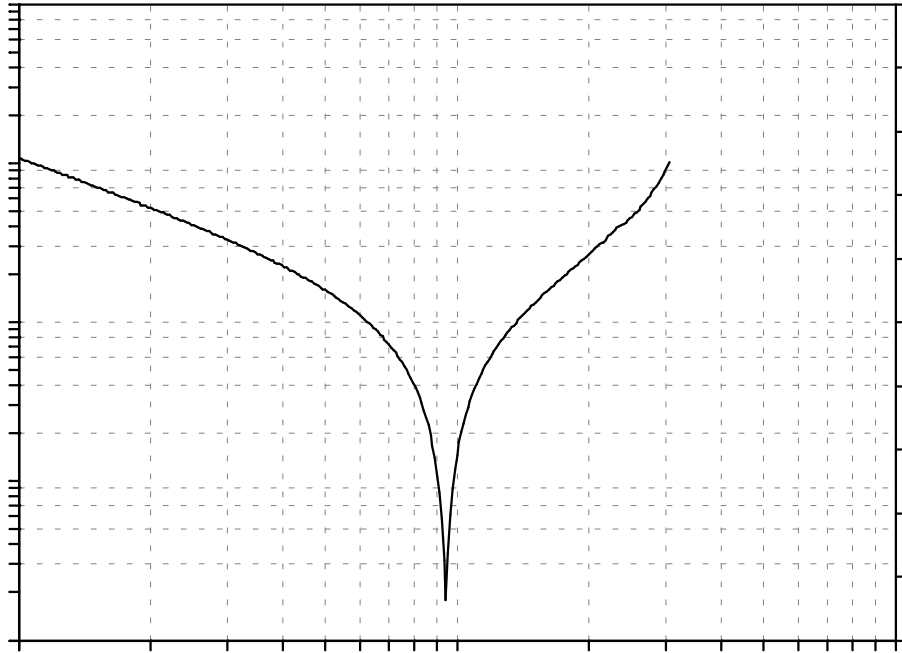
## 2.2 GROSS RESISTANCE AND ANTENNA SYSTEM BANDWIDTH

The gross resistance,  $R_g$ , and the antenna system bandwidth, BW, were measured for each antenna with the antenna tuned for 60.0 kHz. The system was probed by lifting the ground end of the tuning variometer and inserting the impedance probe between the variometer and ground. The gross resistance includes the radiation resistance, tuning system loss resistance, and ground loss resistance. Leakage across the insulators can introduce error in the measurement of  $R_g$  because the low-level measurement signals are not able to heat and eliminate the leakage paths, as the transmitter does under normal broadcast conditions. The gross resistance reported herein was measured during dry weather conditions, and the transmitter was used just prior to the measurement to ensure that leakage paths were dried.  $R_g$  was measured as 0.803 ohm for the primary antenna and 0.913 ohm for the secondary antenna. The higher gross resistance for the secondary antenna is probably attributable to higher ground loss resistance and greater leakage across the antenna toplod and guy wire insulators. The secondary antenna was much more affected by moisture on the insulators and required more time and energy to “dry” them. This indicates that there are tracks and possibly even cracks forming on the surface of the insulators that trap moisture and contribute to leakage paths for the RF energy. The toplod insulators have been in place for over 30 years, and the observed lifetime for that type of insulator has been 30 to 35 years. *The toplod insulators in both antennas should be inspected (as a minimum) and replaced prior to the upgraded high-power broadcast.*

The antenna system bandwidth is the intrinsic bandwidth of the antenna and tuning system, tuned to the operating frequency. The measured values are 263 Hz for the primary antenna and 310 Hz for the secondary antenna.

## 2.3 ANTENNA PARAMETERS

Figures 2 and 3 are raw data plots showing the primary and secondary antenna impedance from 10 kHz to 1 MHz. Tables 2 and 3 list data associated with the figures. The antennas were probed at the copper bus extension from the bushing to the helix, with the helix disconnected. The corona ring was attached to the bus during the measurements. From the plots, one can determine the respective antenna base reactance, the antenna capacitance, the first series resonance, the equivalent download inductance, and the first parallel resonance. Thus, circuit models of each antenna can be constructed that represent the antenna base impedance from DC to as high as 400 kHz. The circuit models illustrate how much antenna capacitance is grouped at the base of the antenna and how much is contained in the toplod, which is useful in determining the actual antenna current.



PHASE (degrees)

**Table 2.** WWVB primary antenna impedance data listing. Page 1 of 3

Frequency (Hz)	Zma (ohms)	Phase (deg)	Frequency (Hz)	Zmag (ohms)	Phase (deg)	Frequency (Hz)	Zmag (ohms)	Phase (deg)
10,000.0	1,068.89	-89.94	16,788.0	630.40	-90.19	28,183.8	355.90	-90.05
10,115.8	1,073.98	-90.22	16,982.4	625.26	-90.07	28,510.2	347.35	-89.95
10,232.9	1,053.90	-90.07	17,179.1	610.90	-89.87	28,840.3	343.68	-90.05
10,351.4	1,033.02	-89.97	17,378.0	607.89	-90.19	29,174.3	341.47	-90.03
10,471.3	1,036.96	-90.27	17,579.2	602.30	-90.06	29,512.1	332.85	-89.94
10,592.5	1,015.76	-90.03	17,782.8	588.83	-89.88	29,853.8	330.20	-90.06
10,715.2	998.80	-90.01	17,988.7	586.35	-90.19	30,199.5	327.28	-90.02
10,839.3	1,002.32	-90.28	18,197.0	580.00	-90.03	30,549.2	319.12	-89.94
10,964.8	979.53	-90.04	18,407.7	567.17	-89.89	30,903.0	316.86	-90.06
11,091.7	963.41	-90.02	18,620.9	565.59	-90.19	31,260.8	313.56	-90.01
11,220.2	966.44	-90.32	18,836.5	558.38	-90.01	31,622.8	305.73	-89.94
11,350.1	945.88	-89.97	19,054.6	546.51	-89.91	31,989.0	303.90	-90.06
11,481.5	931.10	-90.03	19,275.2	545.35	-90.19	32,359.4	300.21	-90.00
11,614.5	933.07	-90.31	19,498.4	537.46	-89.98	32,734.1	292.76	-89.94
11,749.0	910.96	-89.89	19,724.2	526.26	-89.92	33,113.1	291.31	-90.06
11,885.0	898.78	-90.03	19,952.6	525.65	-90.17	33,496.5	287.21	-89.99
12,022.6	900.80	-90.31	20,183.7	517.26	-89.98	33,884.4	280.16	-89.94
12,161.9	878.76	-89.87	20,417.4	506.97	-89.95	34,276.8	279.02	-90.06
12,302.7	868.41	-90.05	20,653.8	506.40	-90.17	34,673.7	274.47	-89.97
12,445.1	869.24	-90.28	20,893.0	498.33	-89.93	35,075.2	267.94	-89.94
12,589.3	847.65	-89.86	21,134.9	488.04	-89.94	35,481.3	267.00	-90.05
12,735.0	838.22	-90.10	21,379.6	487.85	-90.21	35,892.2	262.09	-89.96
12,882.5	837.96	-90.30	21,627.2	478.91	-89.93	36,307.8	256.04	-89.94
13,031.7	817.33	-89.83	21,877.6	469.64	-89.95	36,728.2	255.22	-90.04
13,182.6	809.40	-90.02	22,130.9	469.69	-90.15	37,153.5	250.14	-89.95
13,335.2	808.47	-90.23	22,387.2	460.49	-89.95	37,583.7	244.45	-89.94
13,489.6	789.72	-89.81	22,646.4	452.49	-89.97	38,018.9	243.68	-90.03
13,645.8	781.04	-90.11	22,908.7	452.22	-90.11	38,459.2	238.43	-89.93
13,803.8	779.96	-90.21	23,173.9	443.03	-89.94	38,904.5	233.17	-89.93
13,963.7	761.12	-89.84	23,442.3	435.85	-90.05	39,355.0	232.42	-90.02
14,125.4	754.39	-90.14	23,713.7	434.83	-90.17	39,810.7	227.02	-89.92
14,288.9	751.90	-90.18	23,988.3	425.22	-90.03	40,271.7	222.22	-89.93
14,454.4	733.47	-89.84	24,266.1	418.99	-90.04	40,738.0	221.41	-90.01
14,621.8	727.71	-90.15	24,547.1	417.69	-89.96	41,209.8	215.89	-89.90
14,791.1	724.66	-90.17	24,831.3	408.46	-90.06	41,686.9	211.53	-89.93
14,962.4	707.48	-89.84	25,118.9	403.36	-90.09	42,169.7	210.61	-89.99
15,135.6	702.13	-90.15	25,409.7	401.81	-90.04	42,658.0	205.15	-89.89
15,310.9	698.62	-90.15	25,704.0	392.83	-89.97	43,151.9	201.02	-89.92
15,488.2	682.13	-89.85	26,001.6	387.39	-90.04	43,651.6	200.03	-89.98
15,667.5	677.32	-90.16	26,302.7	386.21	-90.08	44,157.0	194.61	-89.87
15,848.9	673.42	-90.12	26,607.3	377.10	-89.95	44,668.4	190.79	-89.91
16,032.5	657.55	-89.87	26,915.3	372.46	-90.03	45,185.6	189.67	-89.96
16,218.1	653.60	-90.18	27,227.0	370.84	-90.06	45,708.8	184.32	-89.85
16,405.9	648.84	-90.09	27,542.3	362.01	-89.95	46,238.1	180.78	-89.90
16,595.9	633.90	-89.87	27,861.2	357.89	-90.04	46,773.5	179.53	-89.94

**Table 2.** WWVB primary antenna impedance data listing. Page 2 of 3

Frequency (Hz)	Zma (ohms)	Phase (deg)	Frequency (Hz)	Zmag (ohms)	Phase (deg)	Frequency (Hz)	Zmag (ohms)	Phase (deg)
47,315.1	174.18	-89.83	79,432.8	41.59	-88.15	133,352.1	92.83	87.62
47,863.0	171.02	-89.89	80,352.6	39.31	-88.05	134,896.3	95.69	87.82
48,417.2	169.55	-89.91	81,283.1	36.11	-87.71	136,458.3	99.07	87.80
48,977.9	164.31	-89.80	82,224.3	33.34	-87.54	138,038.4	103.77	87.72
49,545.0	161.44	-89.88	83,176.4	30.93	-87.32	139,636.8	106.55	87.87
50,118.7	159.75	-89.88	84,139.5	27.81	-86.86	141,253.8	110.07	87.84
50,699.1	154.68	-89.77	85,113.8	25.08	-86.54	142,889.4	114.99	87.76
51,286.1	152.00	-89.86	86,099.4	22.53	-86.08	144,544.0	117.75	87.91
51,880.0	150.12	-89.85	87,096.4	19.50	-85.30	146,217.7	121.71	87.84
52,480.7	145.20	-89.74	88,104.9	16.78	-84.55	147,910.8	126.64	87.80
53,088.4	142.77	-89.84	89,125.1	14.12	-83.38	149,623.6	129.46	87.93
53,703.2	140.67	-89.81	90,157.1	11.19	-81.45	151,356.1	133.74	87.85
54,325.0	135.89	-89.71	91,201.1	8.47	-78.56	153,108.7	138.89	87.80
54,954.1	133.72	-89.81	92,257.1	5.79	-72.76	154,881.7	141.77	87.93
55,590.4	131.36	-89.77	93,325.4	3.17	-56.90	156,675.1	146.38	87.84
56,234.1	126.76	-89.66	94,406.1	1.78	5.47	158,489.3	151.65	87.76
56,885.3	124.76	-89.79	95,499.3	3.50	59.26	160,324.5	154.74	87.92
57,544.0	122.14	-89.72	96,605.1	6.11	72.91	162,181.0	159.78	87.81
58,210.3	117.76	-89.63	97,723.7	8.96	77.82	164,059.0	165.42	87.79
58,884.4	115.89	-89.76	98,855.3	11.83	80.67	165,958.7	168.48	87.90
59,566.2	112.93	-89.69	100,000.0	14.56	82.43	167,880.4	174.05	87.79
60,000.0	110.78	-89.43	101,157.9	17.48	83.51	169,824.4	179.91	87.77
60,953.7	107.25	-89.63	102,329.3	20.44	84.28	171,790.8	183.19	87.86
61,659.5	104.18	-89.54	103,514.2	23.14	85.01	173,780.1	189.30	87.75
62,373.5	100.28	-89.48	104,712.9	26.22	85.31	175,792.4	195.38	87.75
63,095.7	98.59	-89.59	105,925.4	29.21	85.76	177,827.9	198.96	87.83
63,826.3	95.32	-89.47	107,151.9	31.87	86.16	179,887.1	205.80	87.70
64,565.4	91.69	-89.41	108,392.7	35.15	86.25	181,970.1	212.15	87.71
65,313.1	89.97	-89.51	109,647.8	38.12	86.52	184,077.2	216.10	87.78
66,069.3	86.62	-89.36	110,917.5	40.79	86.77	186,208.7	223.74	87.65
66,834.4	83.17	-89.30	112,201.8	44.24	86.76	188,364.9	230.48	87.66
67,608.3	81.47	-89.40	113,501.1	47.20	86.98	190,546.1	234.92	87.71
68,391.2	78.04	-89.23	114,815.4	49.89	87.14	192,752.5	243.58	87.57
69,183.1	74.76	-89.18	116,144.9	53.51	87.09	194,984.5	250.86	87.57
69,984.2	72.97	-89.26	117,489.8	56.45	87.28	197,242.3	256.20	87.58
70,794.6	69.53	-89.07	118,850.2	59.20	87.40	199,526.2	266.21	87.38
71,614.3	66.40	-89.03	120,226.4	63.06	87.31	201,836.6	274.33	87.30
72,443.6	64.51	-89.08	121,618.6	65.96	87.48	204,173.8	280.68	87.19
73,282.5	61.10	-88.87	123,026.9	68.80	87.55	206,538.0	292.19	86.78
74,131.0	58.12	-88.82	124,451.5	72.89	87.44	208,929.6	301.27	86.54
74,989.4	56.08	-88.84	125,892.5	75.78	87.58	211,348.9	308.35	85.84
75,857.8	52.73	-88.60	127,350.3	78.81	87.56	213,796.2	315.48	84.89
76,736.1	49.85	-88.55	128,825.0	83.15	87.26	216,271.9	318.16	85.66
77,624.7	47.69	-88.51	130,316.7	85.31	87.20	218,776.2	328.53	86.55
78,523.6	44.41	-88.24	131,825.7	88.23	87.61	221,309.5	346.78	86.20

**Table 2.** WWVB primary antenna impedance data listing. Page 3 of 3

Frequency (Hz)	Zma (ohms)	Phase (deg)	Frequency (Hz)	Zmag (ohms)	Phase (deg)	Frequency (Hz)	Zmag (ohms)	Phase (deg)
223,872.1	358.18	85.60	375,837.4	1,998.36	-52.23	630,957.3	251.30	-90.12
226,464.4	368.18	84.85	380,189.4	1,722.63	-56.66	638,263.5	222.40	-90.68
229,086.8	382.51	84.05	384,591.8	1,476.02	-59.93	645,654.2	192.83	-91.04
231,739.5	390.18	83.37	389,045.1	1,276.40	-62.35	653,130.6	165.94	-89.54
234,422.9	397.70	82.75	393,550.1	1,117.45	-64.06	660,693.4	135.96	-90.53
237,137.4	409.75	82.21	398,107.2	987.44	-64.10	668,343.9	103.99	-90.71
239,883.3	415.39	82.04	402,717.0	886.62	-65.87	676,083.0	71.19	-86.11
242,661.0	423.61	81.97	407,380.3	790.64	-67.48	683,911.6	32.11	-86.10
245,470.9	437.58	81.97	412,097.5	693.02	-70.32	691,831.0	13.70	67.15
248,313.3	446.61	82.18	416,869.4	571.12	-72.92	699,842.0	70.46	85.79
251,188.6	459.25	82.30	421,696.5	441.78	-74.47	707,945.8	140.14	84.03
254,097.3	478.34	82.35	426,579.5	301.44	-72.02	716,143.4	241.75	84.84
257,039.6	491.26	82.47	431,519.1	125.23	-58.42	724,436.0	415.12	87.68
260,016.0	508.97	82.48	436,515.8	210.14	52.55	732,824.5	727.78	83.31
263,026.8	532.20	82.40	441,570.4	651.01	51.61	741,310.2	1,737.24	81.98
266,072.5	549.13	82.41	446,683.6	1,406.07	25.37	749,894.2	13,687.2	-51.42
269,153.5	571.82	82.25	451,855.9	1,657.80	-22.15	758,577.6	1,766.33	-84.83
272,270.1	600.70	82.03	457,088.2	1,157.42	-45.02	767,361.5	970.01	-87.93
275,422.9	621.62	81.88	462,381.0	891.35	-48.51	776,247.1	690.50	-88.31
278,612.1	651.20	81.58	467,735.1	790.58	-50.40	785,235.6	515.06	-92.92
281,838.3	685.81	81.27	473,151.3	692.35	-51.66	794,328.2	433.91	-87.65
285,101.8	713.27	81.04	478,630.1	668.77	-50.00	803,526.1	358.80	-87.28
288,403.2	752.78	80.62	484,172.4	632.00	-55.75	812,830.5	285.30	-88.75
291,742.7	798.06	80.18	489,778.8	578.04	-64.38	822,242.6	255.16	-77.80
295,120.9	836.43	79.75	495,450.2	282.39	-21.47	831,763.8	231.64	-71.98
298,538.3	891.33	79.11	501,187.2	538.31	-47.34	841,395.1	213.57	-69.27
301,995.2	952.06	78.42	506,990.7	401.10	-49.79	851,138.0	225.16	-61.64
305,492.1	1,008.36	77.68	512,861.4	316.05	-35.18	860,993.8	205.89	-62.09
309,029.5	1,088.43	76.69	518,800.0	173.13	-12.76	870,963.6	173.27	-58.44
312,607.9	1,177.13	75.58	524,807.5	516.32	17.91	881,048.9	175.19	-37.38
316,227.8	1,266.59	74.31	530,884.4	791.15	14.30	891,250.9	231.00	-21.39
319,889.5	1,393.41	72.63	537,031.8	1,442.23	-2.69	901,571.1	369.98	-30.93
323,593.7	1,536.47	70.63	543,250.3	1,645.80	-41.83	912,010.8	439.94	-53.79
327,340.7	1,693.17	68.20	549,540.9	1,283.57	-66.84	922,571.4	351.83	-72.31
331,131.1	1,916.14	64.96	555,904.3	980.39	-75.08	933,254.3	277.71	-79.62
334,965.4	2,177.94	60.78	562,341.3	830.92	-80.86	944,060.9	240.21	-79.63
338,844.2	2,483.29	55.28	568,852.9	707.10	-85.14	954,992.6	180.15	-82.53
342,767.8	2,904.67	47.61	575,439.9	607.42	-87.50	966,050.9	96.91	-72.30
346,736.9	3,356.79	37.10	582,103.2	528.06	-88.66	977,237.2	382.05	-47.85
350,751.9	3,749.30	23.12	588,843.7	471.74	-89.23	988,553.1	220.54	-71.94
354,813.4	3,974.91	5.96	595,662.1	424.73	-89.62	1,000,000.0	179.09	-71.14
358,921.9	3,787.39	-11.54	602,559.6	379.42	-90.20			
363,078.1	3,319.12	-26.59	609,536.9	344.83	-89.99			
367,282.3	2,838.16	-38.10	616,595.0	311.81	-90.41			
371,535.2	2,376.88	-46.29	623,734.8	278.73	-90.79			

**Table 3.** WWVB secondary antenna impedance data listing. Page 1 of 3

Frequency (Hz)	Zmag (ohms)	Phase (deg)	Frequency (Hz)	Zmag (ohms)	Phase (deg)	Frequency (Hz)	Zmag (ohms)	Phase (deg)
10,000.0	1,077.24	-89.99	16,788.0	636.14	-90.25	28,183.8	353.71	-89.89
10,115.8	1,076.30	-90.30	16,982.4	618.47	-89.78	28,510.2	345.80	-89.90
10,232.9	1,041.94	-89.88	17,179.1	611.69	-90.12	28,840.3	347.67	-90.05
10,351.4	1,041.72	-90.12	17,378.0	613.29	-90.21	29,174.3	339.26	-89.87
10,471.3	1,037.59	-90.26	17,579.2	595.90	-89.78	29,512.1	331.83	-89.90
10,592.5	1,004.24	-89.91	17,782.8	590.09	-90.15	29,853.8	333.56	-90.04
10,715.2	1,006.18	-90.15	17,988.7	590.82	-90.18	30,199.5	325.11	-89.87
10,839.3	1,000.05	-90.22	18,197.0	573.73	-89.78	30,549.2	318.34	-89.90
10,964.8	968.33	-89.79	18,407.7	569.08	-90.16	30,903.0	319.95	-90.03
11,091.7	972.10	-90.25	18,620.9	569.30	-90.15	31,260.8	311.36	-89.88
11,220.2	964.48	-90.21	18,836.5	552.49	-89.78	31,622.8	305.20	-89.90
11,350.1	935.33	-89.75	19,054.6	549.03	-90.19	31,989.0	306.56	-90.01
11,481.5	939.73	-90.28	19,275.2	548.01	-90.12	32,359.4	297.96	-89.86
11,614.5	931.05	-90.15	19,498.4	531.92	-89.77	32,734.1	292.43	-89.91
11,749.0	902.33	-89.79	19,724.2	529.24	-90.18	33,113.1	293.64	-90.00
11,885.0	908.11	-90.41	19,952.6	527.56	-90.08	33,496.5	285.01	-89.84
12,022.6	896.75	-90.09	20,183.7	512.01	-89.79	33,884.4	280.09	-89.91
12,161.9	871.18	-89.77	20,417.4	510.20	-90.18	34,276.8	280.91	-89.99
12,302.7	877.06	-90.42	20,653.8	508.09	-90.07	34,673.7	272.43	-89.84
12,445.1	864.08	-90.03	20,893.0	492.70	-89.76	35,075.2	268.07	-89.91
12,589.3	841.16	-89.77	21,134.9	491.44	-90.22	35,481.3	268.52	-89.97
12,735.0	847.92	-90.49	21,379.6	488.87	-89.97	35,892.2	260.22	-89.81
12,882.5	833.77	-89.87	21,627.2	473.75	-89.75	36,307.8	256.41	-89.91
13,031.7	811.23	-89.93	21,877.6	473.70	-90.21	36,728.2	256.45	-89.95
13,182.6	817.03	-90.56	22,130.9	470.24	-89.99	37,153.5	248.27	-89.82
13,335.2	802.83	-89.92	22,387.2	456.09	-89.84	37,583.7	245.05	-89.91
13,489.6	782.79	-89.85	22,646.4	456.59	-90.18	38,018.9	244.61	-89.93
13,645.8	791.05	-90.43	22,908.7	451.82	-90.00	38,459.2	236.58	-89.80
13,803.8	773.58	-89.82	23,173.9	438.23	-89.80	38,904.5	234.12	-89.91
13,963.7	756.39	-89.89	23,442.3	440.10	-90.18	39,355.0	233.02	-89.91
14,125.4	762.37	-90.41	23,713.7	434.28	-89.89	39,810.7	225.22	-89.78
14,288.9	745.27	-89.84	23,988.3	422.34	-89.69	40,271.7	223.40	-89.92
14,454.4	730.64	-89.96	24,266.1	424.18	-90.34	40,738.0	221.69	-89.88
14,621.8	735.91	-90.38	24,547.1	417.93	-90.05	41,209.8	214.21	-89.77
14,791.1	718.22	-89.81	24,831.3	405.84	-89.77	41,686.9	212.84	-89.92
14,962.4	704.93	-89.98	25,118.9	408.08	-90.16	42,169.7	210.65	-89.85
15,135.6	709.96	-90.34	25,409.7	401.63	-90.01	42,658.0	203.45	-89.75
15,310.9	692.31	-89.81	25,704.0	389.41	-89.96	43,151.9	202.54	-89.91
15,488.2	680.36	-89.99	26,001.6	391.55	-90.08	43,651.6	199.84	-89.82
15,667.5	684.72	-90.33	26,302.7	385.03	-89.92	44,157.0	193.01	-89.74
15,848.9	667.22	-89.82	26,607.3	374.57	-89.88	44,668.4	192.43	-89.89
16,032.5	656.36	-90.02	26,915.3	376.63	-90.11	45,185.6	189.27	-89.80
16,218.1	660.25	-90.29	27,227.0	369.34	-89.91	45,708.8	182.78	-89.71
16,405.9	642.10	-89.78	27,542.3	359.95	-89.90	46,238.1	182.48	-89.88
16,595.9	633.95	-90.09	27,861.2	362.07	-90.08	46,773.5	178.84	-89.74

**Table 3.** WWVB secondary antenna impedance data listing. Page 2 of 3

Frequency (Hz)	Zmag (ohms)	Phase (deg)	Frequency (Hz)	Zmag (ohms)	Phase (deg)	Frequency (Hz)	Zmag (ohms)	Phase (deg)
47,315.1	172.87	-89.70	79,432.8	42.31	-87.81	133,352.1	91.13	87.38
47,863.0	172.67	-89.85	80,352.6	39.56	-87.61	134,896.3	93.20	87.63
48,417.2	168.78	-89.72	81,283.1	36.23	-87.18	136,458.3	97.32	87.43
48,977.9	163.19	-89.67	82,224.3	34.06	-87.17	138,038.4	101.51	87.48
49,545.0	162.98	-89.82	83,176.4	31.27	-86.75	139,636.8	103.64	87.70
50,118.7	158.89	-89.67	84,139.5	28.03	-86.29	141,253.8	108.40	87.45
50,699.1	153.73	-89.67	85,113.8	25.81	-86.09	142,889.4	112.26	87.59
51,286.1	153.46	-89.80	86,099.4	22.94	-85.37	144,544.0	114.58	87.66
51,880.0	149.18	-89.64	87,096.4	19.90	-84.56	146,217.7	119.61	87.51
52,480.7	144.54	-89.63	88,104.9	17.45	-83.78	147,910.8	123.54	87.60
53,088.4	144.22	-89.74	89,125.1	14.64	-82.47	149,623.6	125.79	87.71
53,703.2	139.54	-89.60	90,157.1	11.74	-80.21	151,356.1	131.17	87.51
54,325.0	135.37	-89.58	91,201.1	9.08	-76.69	153,108.7	135.56	87.53
54,954.1	134.99	-89.71	92,257.1	6.31	-70.75	154,881.7	137.69	87.48
55,590.4	130.20	-89.53	93,325.4	3.87	-57.66	156,675.1	142.90	87.26
56,234.1	126.34	-89.53	94,406.1	2.10	-14.15	158,489.3	146.63	87.48
56,885.3	125.89	-89.66	95,499.3	3.17	48.29	160,324.5	149.23	87.70
57,544.0	121.13	-89.52	96,605.1	5.69	67.60	162,181.0	155.72	87.57
58,210.3	117.56	-89.48	97,723.7	8.51	74.90	164,059.0	160.02	87.69
58,884.4	116.87	-89.62	98,855.3	11.18	78.36	165,958.7	162.63	87.77
59,566.2	111.97	-89.48	100,000.0	13.78	80.53	167,880.4	169.59	87.61
60,000.0	110.77	-89.30	101,157.9	16.91	81.75	169,824.4	173.57	87.73
60,953.7	108.10	-89.47	102,329.3	19.56	83.02	171,790.8	176.65	87.81
61,659.5	103.40	-89.28	103,514.2	22.34	83.76	173,780.1	184.29	87.62
62,373.5	100.40	-89.37	104,712.9	25.64	84.24	175,792.4	188.65	87.73
63,095.7	99.26	-89.41	105,925.4	28.27	84.97	177,827.9	191.52	87.77
63,826.3	94.71	-89.17	107,151.9	31.01	85.38	179,887.1	200.07	87.55
64,565.4	91.85	-89.26	108,392.7	34.49	85.49	181,970.1	204.08	87.70
65,313.1	90.55	-89.32	109,647.8	36.99	85.94	184,077.2	207.79	87.73
66,069.3	86.12	-89.06	110,917.5	39.64	86.10	186,208.7	217.18	87.52
66,834.4	83.53	-89.18	112,201.8	43.38	86.26	188,364.9	221.20	87.68
67,608.3	81.91	-89.23	113,501.1	45.69	86.60	190,546.1	225.77	87.64
68,391.2	77.65	-88.94	114,815.4	48.62	86.65	192,752.5	236.04	87.45
69,183.1	75.10	-89.04	116,144.9	52.48	86.55	194,984.5	240.39	87.58
69,984.2	73.39	-89.02	117,489.8	54.79	86.97	197,242.3	246.30	87.47
70,794.6	69.26	-88.75	118,850.2	57.82	86.96	199,526.2	257.55	87.18
71,614.3	67.00	-88.87	120,226.4	61.79	86.82	201,836.6	262.21	87.19
72,443.6	64.76	-88.74	121,618.6	63.98	87.20	204,173.8	269.14	86.82
73,282.5	60.87	-88.55	123,026.9	67.23	87.15	206,538.0	280.76	86.20
74,131.0	58.80	-88.66	124,451.5	71.25	87.14	208,929.6	283.40	85.97
74,989.4	56.42	-88.51	125,892.5	73.46	87.42	211,348.9	288.34	85.84
75,857.8	52.59	-88.28	127,350.3	76.93	87.26	213,796.2	298.20	85.78
76,736.1	50.50	-88.26	128,825.0	81.05	87.32	216,271.9	302.02	86.68
77,624.7	47.97	-88.02	130,316.7	83.21	87.52	218,776.2	313.37	87.14
78,523.6	44.44	-87.79	131,825.7	86.96	87.35	221,309.5	332.38	86.92

**Table 3.** WWVB secondary antenna impedance data listing. Page 3 of 3

Frequency (Hz)	Zmag (ohms)	Phase (deg)	Frequency (Hz)	Zmag (ohms)	Phase (deg)	Frequency (Hz)	Zmag (ohms)	Phase (deg)
223,872.1	341.77	86.61	375,837.4	3,982.24	13.50	630,957.3	1,448.70	-37.47
226,464.4	355.77	85.84	380,189.4	3,933.35	-9.12	638,263.5	1,120.97	-46.09
229,086.8	375.30	84.54	384,591.8	3,370.89	-28.12	645,654.2	5,818.41	-31.40
231,739.5	380.77	82.95	389,045.1	2,664.36	-42.76	653,130.6	2,269.50	-126.17
234,422.9	384.66	81.41	393,550.1	2,110.82	-51.89	660,693.4	1,200.49	-125.35
237,137.4	391.03	80.82	398,107.2	1,675.73	-55.38	668,343.9	844.09	-121.59
239,883.3	389.48	81.14	402,717.0	1,476.79	-60.79	676,083.0	678.97	-116.42
242,661.0	397.80	81.52	407,380.3	1,211.39	-68.28	683,911.6	563.82	-115.35
245,470.9	413.46	81.83	412,097.5	923.61	-74.40	691,831.0	497.62	-109.25
248,313.3	420.02	82.32	416,869.4	675.63	-76.08	699,842.0	445.80	-105.85
251,188.6	435.86	82.43	421,696.5	507.68	-75.88	707,945.8	387.64	-107.01
254,097.3	456.82	82.49	426,579.5	301.93	-77.16	716,143.4	349.44	-99.63
257,039.6	467.61	82.70	431,519.1	98.17	-48.12	724,436.0	302.02	-95.39
260,016.0	489.27	82.52	436,515.8	237.70	51.56	732,824.5	233.42	-88.98
263,026.8	516.90	82.36	441,570.4	598.84	46.19	741,310.2	267.81	-36.94
266,072.5	532.56	82.36	446,683.6	928.52	22.67	749,894.2	724.28	-73.83
269,153.5	564.55	81.94	451,855.9	986.51	5.57	758,577.6	470.25	-100.19
272,270.1	601.36	81.57	457,088.2	960.23	-11.13	767,361.5	397.36	-96.32
275,422.9	632.52	81.26	462,381.0	815.04	-16.13	776,247.1	341.51	-98.94
278,612.1	690.60	80.49	467,735.1	772.89	-14.40	785,235.6	292.76	-102.23
281,838.3	768.78	79.53	473,151.3	808.10	-15.84	794,328.2	278.15	-94.71
285,101.8	884.60	77.87	478,630.1	809.06	-17.84	803,526.1	243.14	-96.82
288,403.2	1,193.07	72.64	484,172.4	903.65	-29.72	812,830.5	207.02	-97.09
291,742.7	2,769.48	32.21	489,778.8	705.79	-49.61	822,242.6	197.78	-85.11
295,120.9	329.03	-66.94	495,450.2	526.19	-41.67	831,763.8	181.29	-82.05
298,538.3	215.99	80.68	501,187.2	410.80	-36.21	841,395.1	172.99	-78.39
301,995.2	396.61	83.57	506,990.7	329.93	-27.35	851,138.0	185.93	-69.56
305,492.1	497.04	83.27	512,861.4	325.06	-4.29	860,993.8	168.23	-71.47
309,029.5	581.30	82.58	518,800.0	252.26	16.23	870,963.6	146.86	-65.35
312,607.9	647.30	82.01	524,807.5	403.82	34.45	881,048.9	154.94	-42.86
316,227.8	703.46	81.39	530,884.4	582.25	42.77	891,250.9	212.14	-29.82
319,889.5	777.00	80.54	537,031.8	860.34	39.80	901,571.1	335.79	-42.47
323,593.7	840.41	79.82	543,250.3	1,052.85	28.95	912,010.8	380.48	-62.71
327,340.7	904.06	79.02	549,540.9	1,273.93	24.18	922,571.4	300.50	-80.22
331,131.1	997.13	77.96	555,904.3	1,587.88	15.42	933,254.3	246.27	-85.67
334,965.4	1,081.96	76.88	562,341.3	1,813.64	-3.06	944,060.9	220.83	-83.79
338,844.2	1,175.65	75.51	568,852.9	1,749.91	-19.25	954,992.6	167.36	-87.14
342,767.8	1,315.65	73.77	575,439.9	1,570.36	-29.94	966,050.9	104.18	-72.89
346,736.9	1,454.20	71.79	582,103.2	1,387.37	-36.36	977,237.2	287.75	-53.54
350,751.9	1,621.11	69.26	588,843.7	1,267.12	-39.62	988,553.1	198.46	-75.86
354,813.4	1,873.18	65.91	595,662.1	1,153.65	-41.37	1,000,000.0	171.65	-75.95
358,921.9	2,148.30	61.31	602,559.6	1,094.79	-40.08			
363,078.1	2,504.86	55.09	609,536.9	1,081.59	-38.96			
367,282.3	3,026.21	45.88	616,595.0	1,097.90	-37.28			
371,535.2	3,582.08	32.74	623,734.8	1,197.86	-35.21			

### 2.3.1 Antenna Capacitance

In the past, VLF and LF antenna capacitance has commonly been measured at low enough frequencies (a few hundred hertz) to minimize the effects of the downlead and other distributed inductances in the antenna. This quantity is called the “static” capacitance. The antenna static capacitance is not to be confused with the topload capacitance, which is only a portion of the static capacitance. Major contributors to the static capacitance are the feedthrough bushing, the pull-off lead, the downlead, the tower, proximity to the helix building, the guy wire insulators, and of course the topload. Most of the capacitances listed above are also distributed within the antenna structure. The technique used for these measurements allows one to assign lumped element equivalent values to the distributed inductances and capacitances that are valid for circuit analysis over a specified frequency range. For example, figure 4(a) shows a simple circuit model of the primary antenna with values assigned for the topload capacitance, the downlead inductance, and the shunt capacitance concentrated at the base of the antenna. The loss resistance is not assigned a value because, in this model, it is dependent on frequency. Figure 4(b) is a similar circuit model of the secondary antenna. Both models are valid for analysis up to about 400 kHz. They are, in fact, better circuit models of each antenna than a simple series resonant circuit because they allow the analyst to determine how much current is actually flowing in the antenna vice the current measured with the current transformer located in the helix house. The antenna shunt capacitance also influences the antenna effective height measurement since the “antenna current” is measured at the ground end of the variometer, which includes the current in the shunt capacitance. In fact, the antenna effective height is approximately 4.2 percent higher than that calculated using the “antenna current” measured by the station’s antenna current monitor! Note from the values in the models how similar the two antennas appear electrically.

### 2.3.2 Antenna Base Reactance

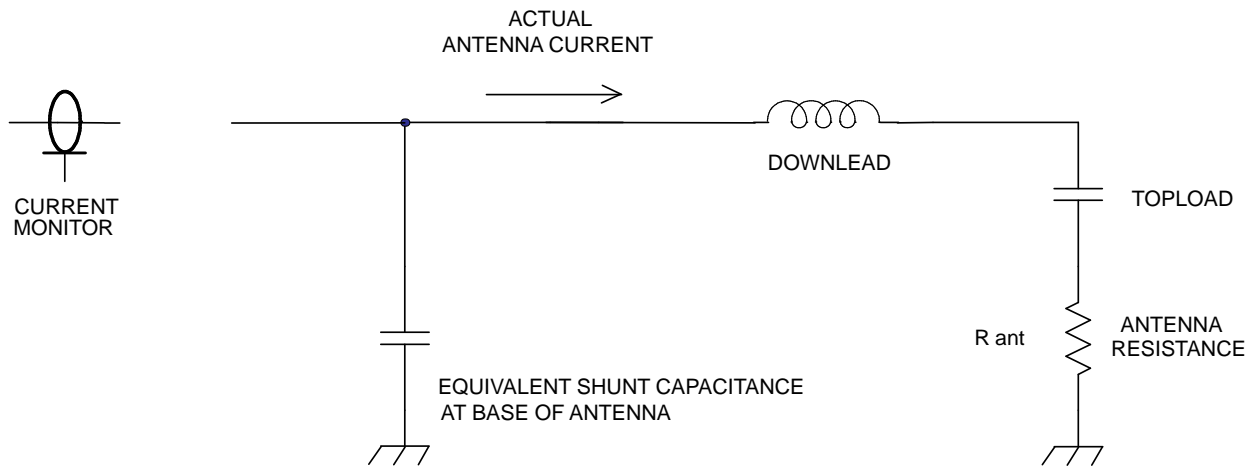
The base impedance of the antenna was measured at the same point as the static capacitance. At 60 kHz, the antenna impedance is almost entirely capacitive reactance. The measured values at 60 kHz are  $-114.9$  ohms for the primary antenna and  $-112.9$  ohms for the secondary antenna.

### 2.3.3 Antenna Resonance

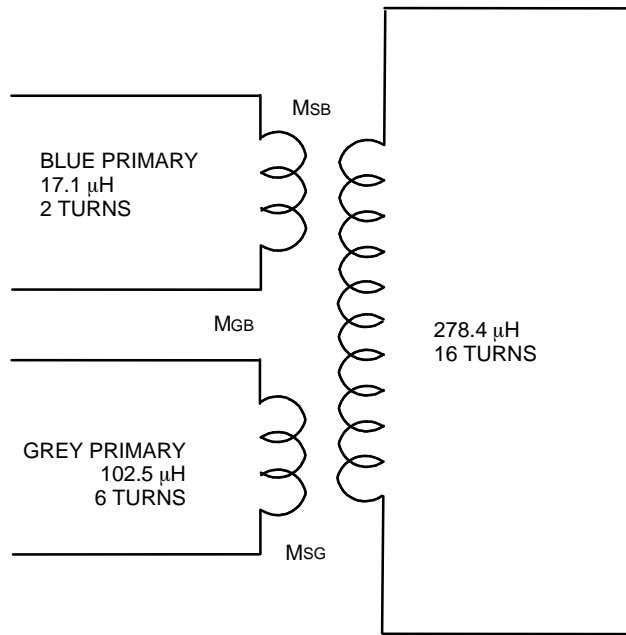
The first series self-resonance of each antenna can be seen as an impedance minimum in figures 2 and 3. The primary antenna’s first series self-resonance is 94.36 kHz, with a total resistance at that frequency of 1.77 ohms, and the secondary antenna’s first series self-resonance is 94.8 kHz, with a total resistance at that frequency of 2.28 ohms. The first parallel self-resonance of each antenna can be seen as an impedance maximum in figures 2 and 3. The primary antenna’s first parallel self-resonance is 356.5 kHz, and the secondary antenna’s first parallel self-resonance is 372.3 kHz.

### 2.3.4 Antenna Downlead Inductance

The downlead is the primary radiator of the RF energy, with inductance and capacitance (to ground) that are distributed in nature, as mentioned in 2.3.1. For the frequency range DC to about 400 kHz, the equivalent downlead inductance is  $208.8 \mu\text{H}$  for the primary antenna and  $208.0 \mu\text{H}$  for the secondary antenna. These values are shown in the antenna model in figure 4.

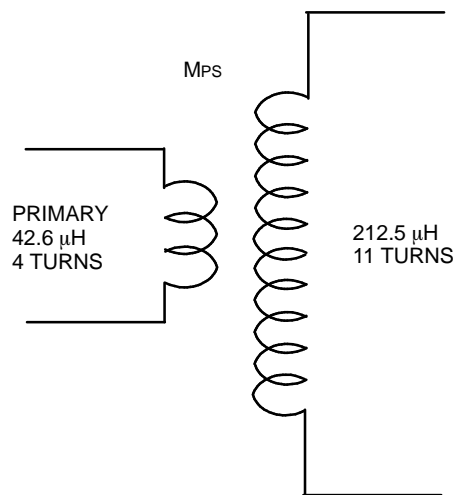


helix is shown in figure 5(b). The primary helix has two primaries so that it can be driven by either the blue or grey power amplifier.



M<sub>SB</sub> = MUTUAL BETWEEN BLUE PRIMARY AND SECONDARY = 20.7 μH  
M<sub>SG</sub> = MUTUAL BETWEEN GREY PRIMARY AND SECONDARY = 18.0 μH  
M<sub>GB</sub> = MUTUAL BETWEEN BLUE AND GREY PRIMARIES = 25.9 μH

(a) primary helix



M<sub>PS</sub> = MUTUAL BETWEEN PRIMARY AND SECONDARY = 42.5 μH

(b) secondary helix

**Figure 5.** Helix circuit models.

## 2.5 ANTENNA TUNING VARIOMETER

The antenna tuning variometers in the primary and secondary helix houses are not identical. The variometer in the primary helix house consists of two strands of parallel 1-inch litz, wound as a rotor *in parallel with* a stator, providing four strands of parallel litz to share the total current. The variometer in the secondary helix house consists of two strands of 1-inch litz, wound as a one-half stator in series with a rotor, in series with the other one-half stator, providing two parallel strands of litz to share the total current. As a result of the way the rotor and stator are connected, the total inductance range of the variometer in the secondary helix house is much greater than the variometer in the primary helix house. Consequently, the secondary helix house provides greater tuning range at the price of greater sensitivity to variometer position. Figure 6(a) plots primary helix house variometer inductance versus position, and figure 6(b) plots secondary helix house variometer inductance versus position.

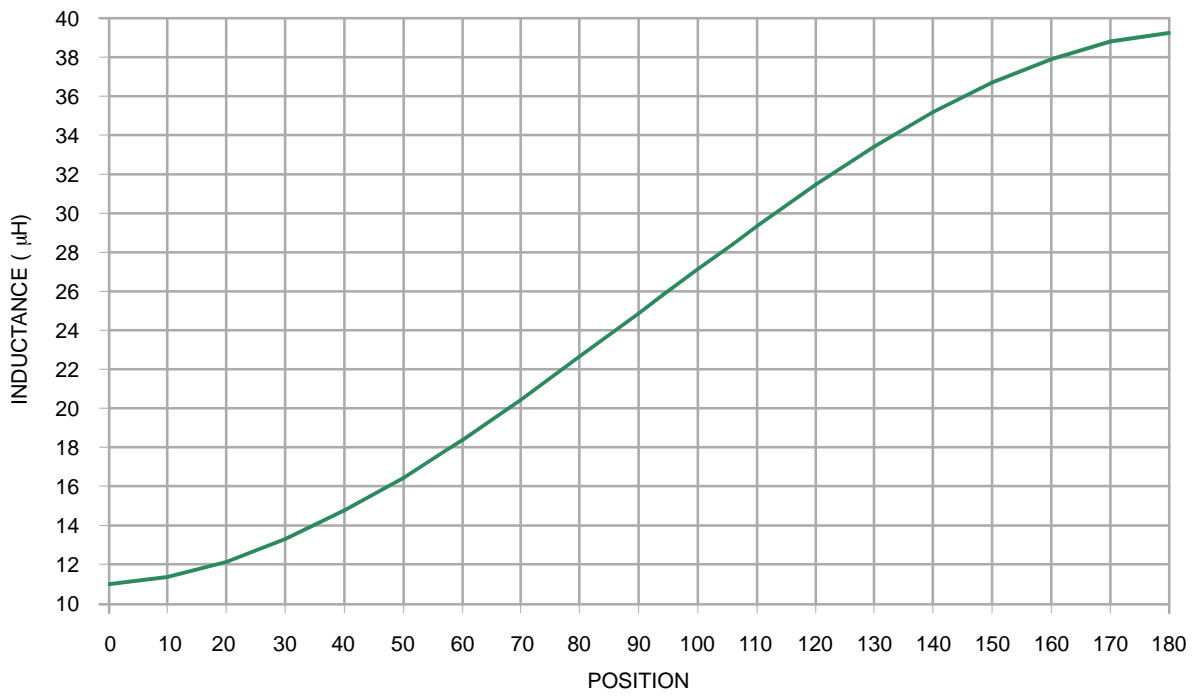
## 2.6 ANTENNA TUNING SYSTEM RESISTANCE

The loss resistance in the antenna tuning system is the loss of the helix and tuning variometer, measured at 60 kHz. The loss was measured by substituting a low-loss capacitor for the antenna when the system is resonated at 60 kHz, measuring the total loss, and subtracting the loss of the capacitor. It is important to probe the antenna tuning system at the same point as the gross resistance is measured (the “ground” end of the variometer) so that the voltage and current distribution is the same through the tuning components and their stray capacitances. The measured values of loss resistance are 0.135 ohm for the primary helix house and 0.130 ohm for the secondary helix house.

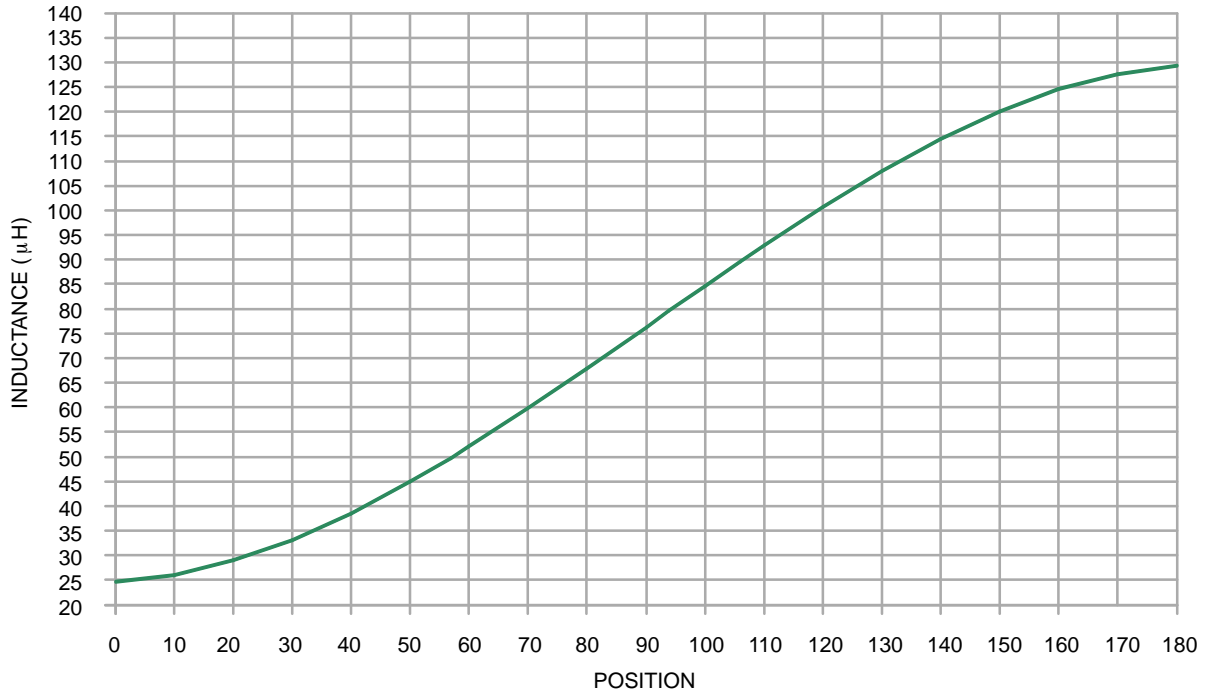
## 2.7 MUTUAL IMPEDANCE BETWEEN ANTENNAS

Electrically small monopole antennas have a maximum radiated power limit determined by the breakdown voltage at some location such as the helix, topload insulators, topload corona limit, or feedthrough bushing. To first order, the maximum radiated power for voltage-limited operation is proportional to topload area squared. Thus, two antennas, electrically close together, can radiate on the order of four times the power of a single antenna. In addition, operation on two antennas divides the total current between two ground and tuning systems, increasing the radiation efficiency. Consequently, we have recommended examining the operation of the two WWVB antennas simultaneously as an array.

To determine the operational parameters for an array, both the self-impedance and mutual impedance must be known. Knowledge of the mutual impedance, especially the resistive part, is important to determine the efficiency of operation as an array. Due to its importance, it was decided to add the measurement of mutual impedance to the test plan. This was done in lieu of near-field measurements under the topload. The near-field measurements were not as important as originally thought for reasons described in 4.4.



(a) primary helix house



(b) secondary helix house

**Figure 6.** Helix house variometer inductance versus position.

Two antennas can be treated as a linear two-port network, and all network theorems including reciprocity apply. A network representation using the open circuit ( $Z$ ) parameters is shown in figure 7.

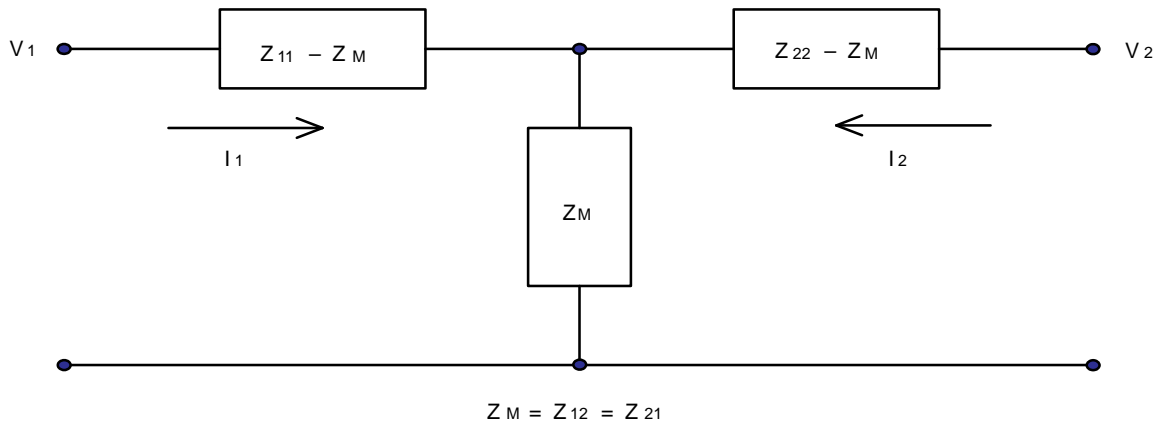


**Figure 7.** Linear two-port network model of two coupled antennas.

The network equations using these parameters are as follows:

$$V_1 = Z_{11}I_1 + Z_{12}I_2 \quad (1)$$

and

$$V_2 = Z_{21}I_1 + Z_{22}I_2 \quad (2)$$

with  $Z_{12} = Z_{21} = Z_m$  from reciprocity.

Normally the magnitude of the mutual is easily measured by driving one port with a known current and measuring the open-circuit voltage.

$$Z_m = \left[ \frac{V_2}{I_1} \right]_{I_2=0} \quad (3)$$

The magnitude of the voltage and current at the two ports is usually easy to measure at low power,

First the resistive values of  $Z_{11}$  and  $Z_{22}$  are accurately measured. For this measurement, the antenna not being measured has to be open-circuited and the coupling winding(s) disconnected. The most accurate measurement of resistance is at zero phase angle so the variometer is tuned for system resonance at the operating frequency, and the total series resistance is measured.

Then an additional measurement is made while feeding one antenna with the other operating as a tuned parasite. This amounts to feeding one port in the network while the opposite port is shorted ( $V_2 = 0$ ). The input impedance ( $Z_{in} = V_1/I_1$ ) of the active antenna is measured. The system of network equations becomes as follows:

$$V_1 = Z_{11}I_1 - Z_m I_2 \quad (4)$$

$$0 = Z_m I_1 - Z_{22} I_2 \quad (5)$$

Solving for  $I_2$  gives the following:

$$I_2 = \frac{Z_m}{Z_{22}} I_1 \quad (6)$$

Note that  $I_2/I_1$  will be maximum when the magnitude of  $Z_{22}$  is minimum. This occurs when  $X_{22} = 0$ , which means that  $Z_{22}$  is real (resistive) and equal to  $R_{22}$ . This condition can be achieved by measuring  $I_1$  and  $I_2$  while tuning the variometer in the parasitic helix house until the ratio is maximum. Tuning the variometer results in changing only the reactive part of  $Z_{22}$ . When the ratio of  $I_2/I_1$  is maximum, then  $Z_{22} = R_{22}$ , which is known from the previous measurement, and the mutual can be determined from the following equation:

$$Z_m = R_{22} \frac{I_2}{I_1} \quad \text{when} \quad \left| \frac{I_2}{I_1} \right| = \max \quad (7)$$

Both the real and imaginary part of the mutual can be determined in this way if the phase between  $I_2$  and  $I_1$  is known. However, as previously discussed, this phase is not known, and this relationship can only be used to determine the magnitude of the mutual impedance as follows.

$$|Z_m| = R_{22} \left| \frac{I_2}{I_1} \right| \quad \text{when} \quad \left| \frac{I_2}{I_1} \right| = \max \quad (8)$$

Determination of the real and imaginary part of  $Z_m$  can be accomplished as follows. We start by subtracting the input impedance with the parasitic active,  $Z_{in}$ , from the open-circuit network impedance (parasitic antenna floating),  $Z_{11}$ .

$$Z_{11} - Z_{in} = \frac{I_2}{I_1} Z_m = \frac{Z_m^2}{Z_{22}} \quad (9)$$

When port 2 is tuned,  $Z_{22} = R_{22}$  and the above equation becomes

$$Z_{11} - Z_{in} = \frac{Z_m^2}{R_{22}} = \frac{(R_m + jX_m)^2}{R_{22}} \quad (10)$$

Therefore,

$$Z_m = R_m + jX_m = \sqrt{R_{22}(Z_{11} - Z_{in})} \quad (11)$$

A procedure was used for measuring the mutual impedance based on the above equations. First  $R_{11}$  and  $R_{22}$  are measured. Then one antenna is fed at low power with the other antenna in a parasitic mode, meaning the antenna is grounded through the helix and tuning variometer. (Note for the WWVB configuration the coupling turns wound around the helix must also be disconnected.) Currents in both antennas were measured using HP 3586 selective-level meters. The variometer in the parasitic helix house is tuned until the ratio of  $I_2/I_1$  is maximum. Communications required for this tuning were provided by hand-held radio. The maximum current ratio is recorded, as is the input impedance when the current ratio is maximum, being careful not to change the parasitic tuning. After this measurement is completed, the parasitic antenna is open-circuited by ungrounding the variometer connection, and the input impedance is measured again. The difference between these two impedances is used as described above to solve for  $R_m$  and  $X_m$ . (Note: Dangerous static charge can build up on an ungrounded antenna. Standard practice is to ground the antenna through a high-value static drain resistor for this measurement.)

For electrically short monopoles such as the WWVB LF antennas, the resistance observed at low power can change rapidly with time due to moisture on the insulators. The amount of this change depends upon the amount of moisture, the number, type and condition of the insulators, and the amount of contamination present on the surface of the insulators. For this reason, it is desirable to make these types of measurements during fair weather; but even then, it is often necessary to “dry” the antenna prior to each measurement by operating the transmitter into the antenna at full power for several minutes prior to making a low-power measurement of resistance. This has been observed to be necessary even in dry weather for many of the antennas we have measured.

The WWVB antennas also exhibited significant differences in resistance before and after “drying,” especially the north (secondary) antenna. The north antenna resistance was higher than the south, exhibiting much more variability and longer “drying” times than the south antenna. This could be attributable to a problem such as surface cracks or tracking on one or more insulators in the north antenna system.

This approach to measuring the mutual requires that the value of resistance in the parasitic antenna ( $R_{11}$  or  $R_{22}$ ) be accurately measured. If the resistance of the parasitic antenna changes, it will lead to errors in the measured value of the mutual. We made the above type of measurements to determine the mutual at low power from both helix houses and were careful to “dry” the parasitic antenna just before measurement. The measurements made from the north antenna (south parasitic) appear to be good in that they are self-consistent. Also, current-ratio-only measurements were made with the transmitter at almost full power (approximately 100 amps antenna current).

The measurements are summarized below in table 4, and figure 8 depicts the circuit model of the WWVB antennas showing the mutual values. Note that the magnitude of  $Z_m$  determined from the current ratio and  $R_{22}$  (equation 8) is essentially the same as the solution from the complex measurements (equation 11). Note also that this current ratio is practically the same as measured using the transmitter at 100 amps. *The estimate for the mutual is taken from the measurements from the north (secondary) helix house with the south (primary) used as the parasitic.*

**Table 4.** WWVB mutual impedance measurement data.

Quantity (measured at 60 kHz)	Units	Value
Current ratio, $I_2/I_1$ , measured at low level	none	0.9279
Current ratio, $I_2/I_1$ , measured with transmitter	none	0.9286
Input impedance with parasitic active, $Z_{in}$	ohms	$1.498 + j0.692$
Input impedance with parasitic floating, $Z_{11}$	ohms	$1.148 + j0.085$
Parasitic side impedance with input side floating, $Z_{22}$	ohms	$0.8085 + j0.090$
Magnitude of mutual impedance, $ Z_m $ (equation 8)	ohms	0.7502
Mutual impedance, $Z_m$ (equation 11)	ohms	$0.7527 \angle -59.98 = 0.3765 - j0.6517$

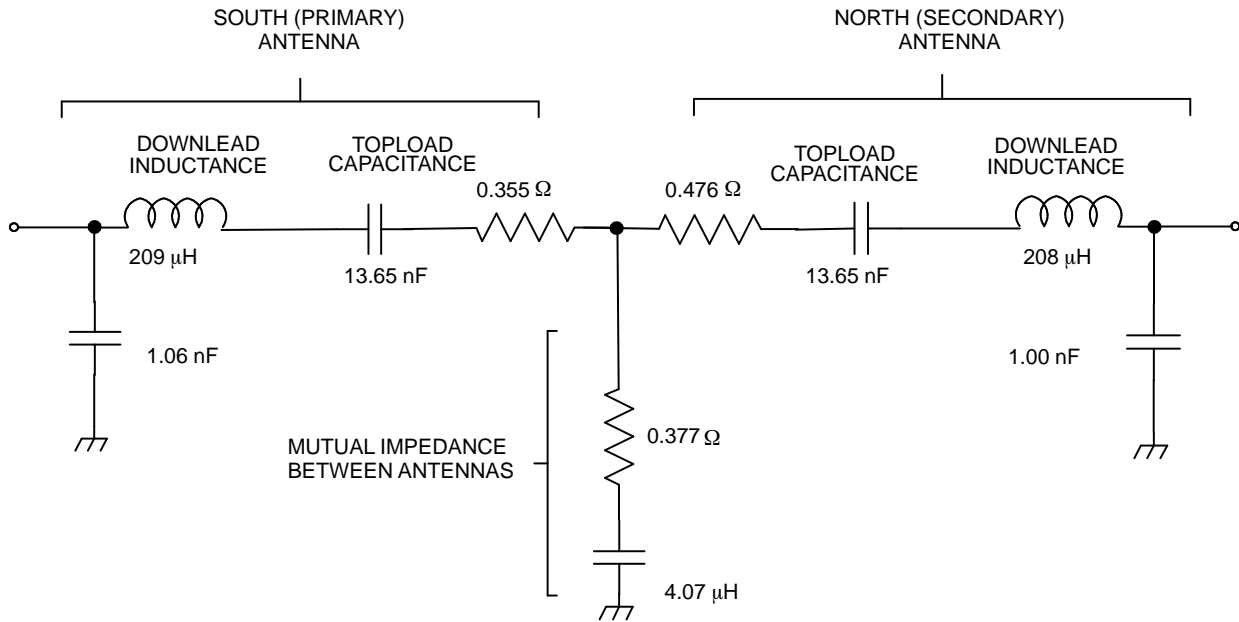


**Figure 8.** Mutual impedance circuit model of antennas (60 kHz).

## 2.8 TRANSMISSION LINES

The electrical parameters of each transmission line were measured at 60 kHz from each helix house by using the network analyzer impedance measurement system. The lines were disconnected from the primary turns on the helix and the impedance measurement system was connected. The lines were measured while terminated in the transmitter building with both an open circuit and short circuit placed on the line inside the transmitter building.

The transmission line is characterized by a characteristic impedance,  $Z_0$ , and a propagation constant  $\gamma = \alpha + j\beta$ . The characteristic impedance of the line (at the measurement frequency) can be determined from the open circuit,  $Z_{open}$ , and short circuit,  $Z_{short}$ , measurements by the following formula:

$$Z_0 = \sqrt{Z_{short} Z_{open}} \quad (12)$$

A formula relating these measurements and the propagation constant times line length can be derived.

$$e^{2\gamma\ell} = e^{2\alpha\ell} e^{2j\beta\ell} = \frac{1 + \sqrt{\frac{Z_{\text{short}}}{Z_{\text{open}}}}}{1 - \sqrt{\frac{Z_{\text{short}}}{Z_{\text{open}}}}} \quad (13)$$

The magnitude of the propagation factor,  $e^{2\gamma\ell}$ , is the two-way line attenuation factor,  $e^{2\alpha\ell}$ , and the phase of the propagation factor,  $2\beta\ell$ , is the round-trip phase shift or twice the electrical length of the line (in radians). The one-way line attenuation factor and phase shift can be found from the following formulas.

$$\alpha\ell = \frac{1}{2} \ln \left| \frac{1 + \sqrt{\frac{Z_{\text{short}}}{Z_{\text{open}}}}}{1 - \sqrt{\frac{Z_{\text{short}}}{Z_{\text{open}}}}} \right| \quad (14)$$

$$\beta\ell = \tan^{-1} \sqrt{\frac{Z_{\text{short}}}{Z_{\text{open}}}} \quad (15)$$

The physical length of the line,  $L$ , can be calculated from the electrical length if one knows the velocity factor,  $v$ . For the air dielectric of the suspended two-wire transmission line, the velocity factor will be very nearly 1.0. Therefore, the physical length of the line may then be calculated as follows:

$$L = v \frac{c}{f} \left( \frac{\beta\ell}{360} \right) \left( 0.3048 \frac{\text{feet}}{\text{meters}} \right) \quad (16)$$

with  $c$  = speed of light =  $3 \times 10^8$  m/s, and  $f$  = 60 kHz.

Then, the calculated physical length of the transmission lines, including helix house and transmitter building segments, is  $L_{\text{pri}} = 1424.7$  feet and  $L_{\text{sec}} = 1443.3$  feet.

The measurements of  $Z_{\text{open}}$  and  $Z_{\text{short}}$  and the parameters derived for both lines using the above formulas are summarized below in table 5.

**Table 5.** Transmission line parameters.

Quantity (measured at 60 kHz)	Units	South (Primary)	North (Backup)
$Z_{\text{SHORT}}$	ohms	317.3 $\angle$ 89.08°	330.5 $\angle$ 88.92°
$Z_{\text{OPEN}}$	ohms	857.6 $\angle$ -91.2°	865.1 $\angle$ -90.85°
$Z_0$	ohms	522	535
Electrical length of line	degrees	31.3	31.7
Total attenuation	dB	0.0094	0.0078
Calculated physical length	feet	1425	1443

As a crosscheck, the characteristic impedance of the line,  $Z_0$ , calculated from the physical measurements (see appendix B) is

$$Z_0 = 120 \ln \left( \frac{\text{separation between wires}}{\text{wire radius}} \right) = 120 \ln \left( \frac{20}{0.247} \right) = 527.3 \ \Omega \quad (17)$$

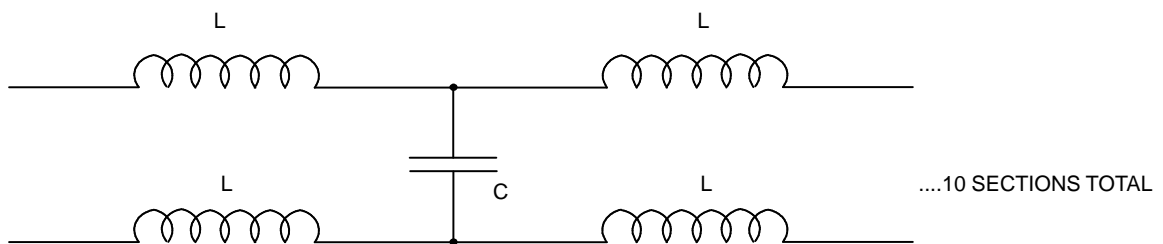
This calculation is based on typical physical dimensions of the transmission line and agrees very closely with the average  $Z_0$  from the electrical measurements.

## 2.9 ANTENNA AND TUNING SYSTEM CIRCUIT MODEL

The preceding paragraphs enable one to construct a circuit model of the antenna and antenna tuning system for the current operating frequency of 60 kHz. A circuit model of this type may be used for computer-assisted system analysis of the WWVB antenna and tuning system, such as tuning optimization, component stress analysis, harmonic transfer analysis, EMP susceptibility analysis, etc. Figures 9 and 10 show circuit models of the primary and secondary transmission systems constructed from the baseline data. The models may be used for many types of computer-aided system analysis from DC to about 400 kHz. However, the loss resistance values for the components and antenna are accurate only at 60 kHz. Figure 11 is an integrated circuit model of both systems, showing the mutual impedance coupling the two antennas measured at 60 kHz.

In figures 9 and 10, it may appear that there is a discrepancy between the measured  $R_g$  and the loss resistances identified in the model. This is not the case when one takes into account the effect of the antenna shunt capacitance on the antenna and ground loss. This loss is “transformed” by the antenna shunt capacitance which, when combined with the tuning inductance loss, adds up to the appropriate  $R_g$  for each antenna and tuning system.

Any lossless balanced transmission line model that has the characteristic impedance and total phase shift (at 60 kHz) shown in the figures may be used for circuit analysis of the model. The transmission line model developed for this report consists of 10 sections of balanced pi-networks as shown below.



Where 
$$L = \frac{\frac{1}{2} Z_0 \left( 1 - \cos \left( \frac{\phi_L}{10} \right) \right)}{\sin \left( \frac{\phi_L}{10} \right)} \frac{1}{2 \pi 60,000} \quad \text{and} \quad C = \frac{\sin \left( \frac{\phi_L}{10} \right)}{2 \pi (60,000) Z_0} \quad (18)$$

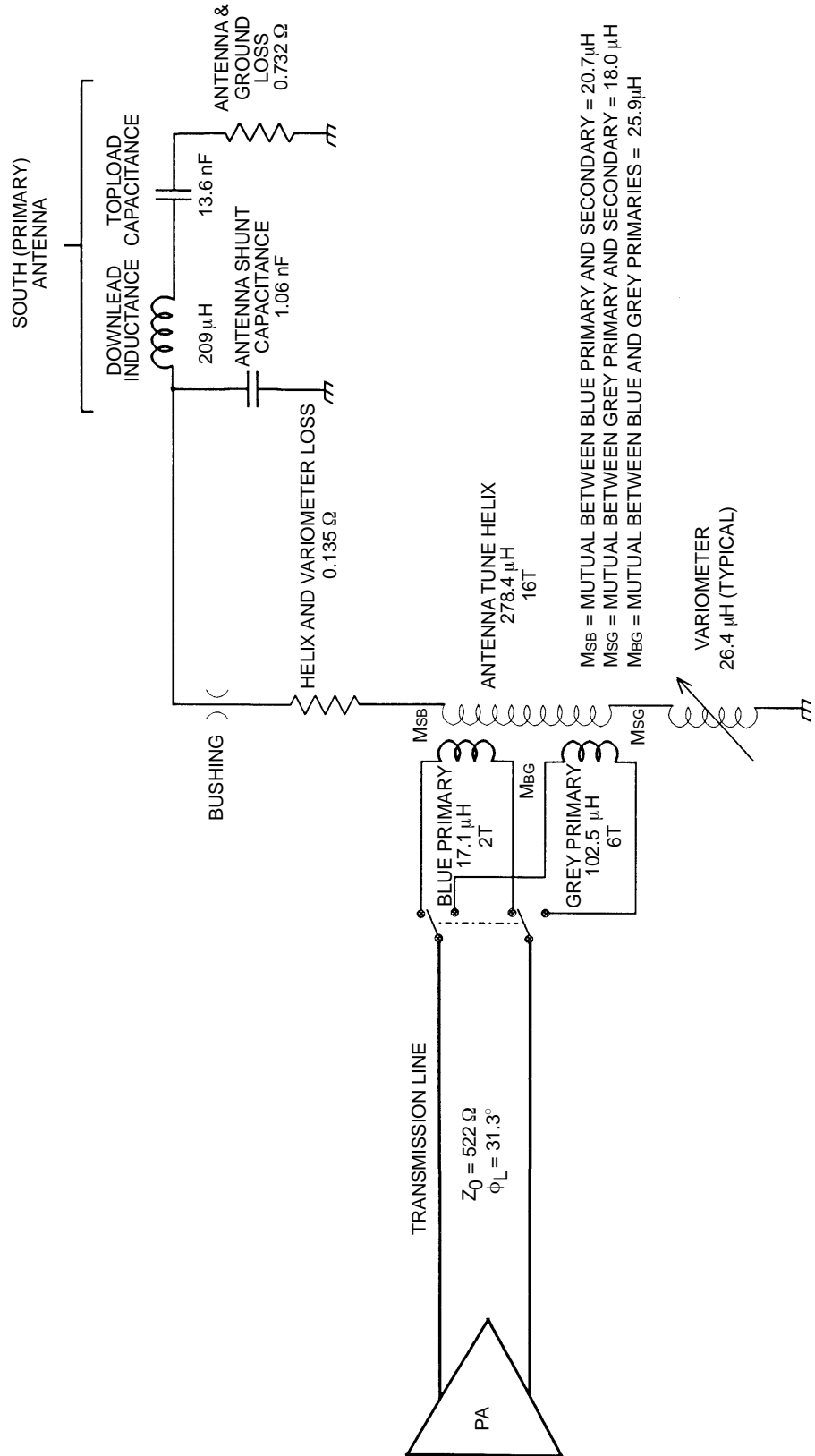
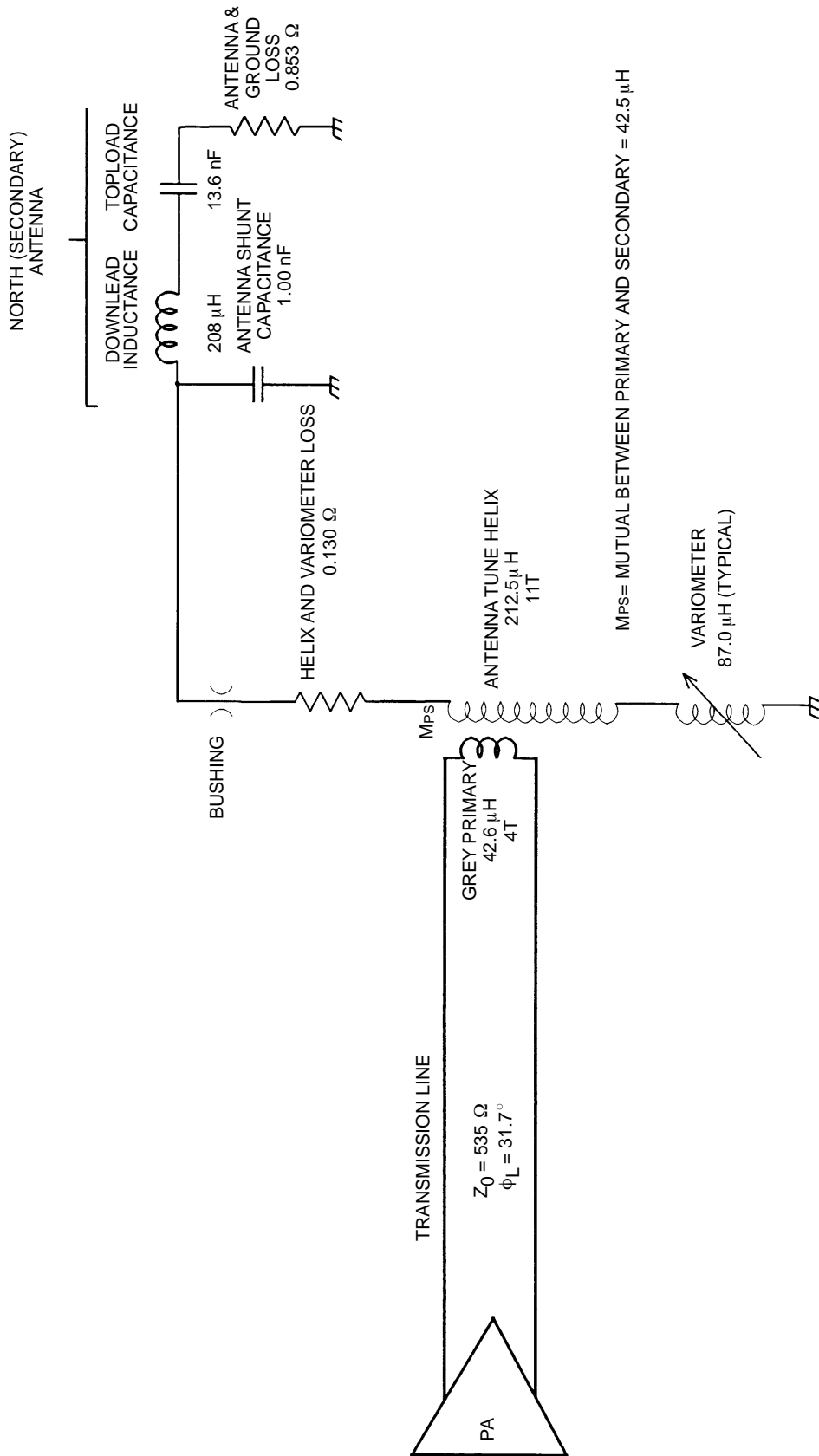


Figure 9. WWVB primary antenna and tuning system circuit model.



**Figure 10.** WWVB secondary antenna and tuning system circuit model.

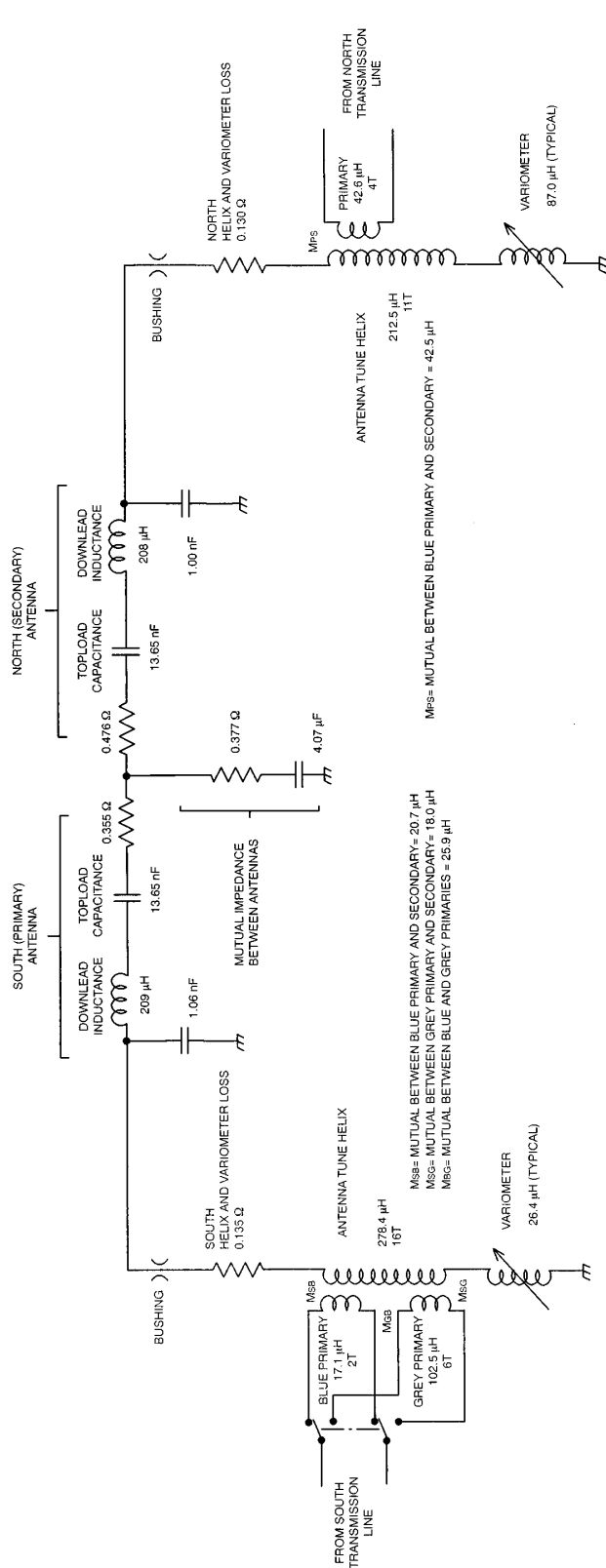


Figure 11. WWVB mutual impedance circuit model.

## 2.10 GROUND CONDUCTIVITY MEASUREMENTS

Ground conductivity measurements were made at seven locations in the vicinity of the WWVB antennas. The measurements were made with a Biddle four-wire ground resistance meter, which operates at approximately 50 Hz, using a Wenner array configuration (Wait & Wahler, 1956). This type of array consists of four stakes equally spaced in a straight line. The measurement consists of driving a current between the outer two stakes and measuring the in-phase component of the voltage induced between the inner two stakes. This ratio of voltage to current is called the mutual resistance and is a measure of the average conductivity in a volume of earth with dimensions on the order of the stake spacing. For an earth with uniform conductivity, the DC mutual resistance,  $r_m$ , as a function of stake spacing,  $s$ , and conductivity,  $\sigma$ , is given in the following formula:

$$r_m = \frac{1}{2\pi\sigma s} \quad (19)$$

This formula is inverted and used to give what is called the apparent conductivity,  $\sigma_{app}$ , for each measurement of  $r_m$  as follows:

$$\sigma_{app} = \frac{1}{2\pi r_m} \quad (20)$$

At each site, a series of measurements of  $r_m$  are taken with different stake spacings. It is convenient to double the stake spacing for each succeeding measurement while keeping the meter and one of the two inner stakes at a fixed location. This allows only two stakes to be moved for each succeeding measurement. We usually start out with the stakes at 1/2-foot spacing doubling out to 64 feet or farther if the conductivity is low. The results are converted to apparent conductivity by the above formula.

Measurements of this type were made at seven locations around the two WWVB antenna systems. Two of these measurements (sites 1 and 2) were taken within the ground radial system of the antennas. The other five sites were well outside of the ground radial system.

Buried wires can disturb the conductivity measurements. If there are buried wires running in the same direction as the measurements, the apparent conductivity will be increased. This effect was observed at sites 1 and 2 where, at the larger stake spacings, the apparent conductivity is greatly enhanced. Therefore, the data from these two sites were discarded.

The measurements at the other five locations have been averaged and are plotted versus stake spacing in figure 12. Included in the figure is the apparent conductivity calculated for the best-fit two-layer model. The average measured curve in the figure fits this simple two-layer model very well.

Formulas for the two-layer model have been taken from Sunde (1949) and the parameters adjusted to fit the average of the measurements. The best fit occurred when using an upper layer 0.45 meter thick with conductivity of 14.5 millimhos per meter and a lower layer with conductivity of 220 millimhos per meter. A plot of the calculated data for this two-layer model is shown in figure 12 and indicates a very good fit. These best-fit data are summarized in table 6 below.

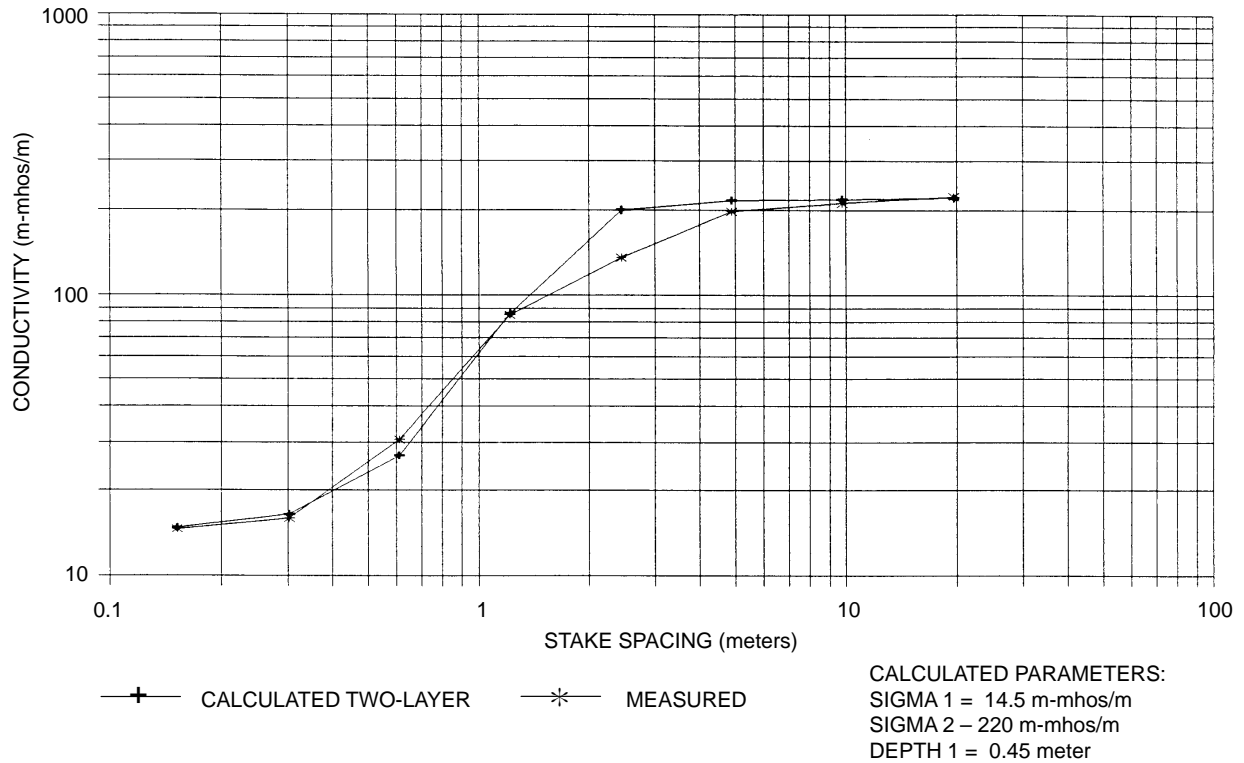


**Figure 12.** Average ground conductivity around WWVB.

**Table 6.** Average ground conductivity.

	Conductivity (millimhos/m)	Thickness (meters)
Top Layer	14.5	0.45
Lower Layer	220	$\infty$ (flat earth)

This conductivity is unusually high, which makes this site an excellent location for VLF/LF antennas in that the ground losses will be low. It is interesting to note that at locations where the ground conductivity is high, such as at Fort Collins, the optimum ground system consists of a greater number of shorter ground wires; whereas, at sites where the conductivity is low, the optimum ground system consists of fewer longer wires.

## 3. EFFECTIVE HEIGHT MEASUREMENTS

### 3.1 BACKGROUND

To provide accurate coverage predictions for LF transmitters, one must have accurate knowledge of the radiated power for use in the propagation prediction programs.

Due in part to the large wavelengths at VLF/LF (6 to 20 km), there is no direct way to measure radiated power. The method used for these measurements consists of an extensive field strength survey in the vicinity of the antenna. The field strength measuring equipment must be accurately calibrated, and the distance to each measurement position must be precisely known. The variation in terrain and conductivity and uncertainty of position gives rise to random errors at each measurement site, which is overcome by averaging the measurements at many sites. Radiated power can also be estimated from distant field strength measurements but with considerably reduced accuracy due to the uncertainty in propagation.

Field strength surveys by helicopter are thought to be the most accurate way of determining radiated power because the measurements are made at an elevation that eliminates terrain effects. The drawbacks are expense and difficulty calibrating the receiving antenna on the helicopter. In places where the terrain is very rough and/or there is no access to ground-based measurement sites, surveys by helicopter are the only way to make measurements accurately. The terrain and access around Fort Collins is acceptable for making ground-based measurements.

### 3.2 CURRENT MONITOR LOCATION

The effective height of an antenna ( $h_e$ ) relates the antenna base current to the distant radiated field. The radiated fields are directly proportional to antenna base current times effective height. The antenna effective height can be determined by monitoring the antenna current during the field strength survey. Given effective height and antenna current, radiated power can be calculated.

The antenna base current for the WWVB antenna would be the current at the outside of the helix house feedthrough bushing. It is difficult to measure the current at that location because it is at high voltage. The current is usually measured on the low side of the helix, which is a low-voltage point. These currents differ slightly due to the shunt capacitance of the helix house tuning elements, bus work, bushing, and tower feed structure. This difference varies with frequency somewhat, being the greatest at the higher frequencies. At WWVB on 60 kHz, this difference was measured on the primary antenna to be about 4 percent.

*Note: The measurements described in this report are all referred to the current measured at the bottom of the helix.*

### 3.3 MEASUREMENTS

The radiated power, antenna effective height, and radiation resistance of the primary WWVB antenna were determined for 60-kHz operation by a field strength survey while at the same time recording antenna current. The effective height of the backup antenna was not measured, but since the primary and backup antennas are identical, the effective height of the backup antenna is assumed to be the same as the primary antenna.

The survey consisted of measurements at various locations around the Fort Collins area and was completed during the first 2 days of the second week of testing. The measurement locations used for this survey are given in terms of range and bearing from the antenna center and are listed in table 7.

**Table 7.** WWVB field strength measurement sites.

<b>10/17/94, Rain and snow conditions</b>					
<b>Site</b>	<b>Time (local)</b>	<b>GPS Mark</b>	<b>Range (yards)</b>	<b>Range (meters)</b>	<b>Bearing<sup>1</sup> (degrees)</b>
1	11:15:30	13	10,097	9,233	84
2	11:33:00	14	9602	8780	78
3	11:56:00	15	10,178	9307	113
4	12:17:00	16	14,448	13,211	107
5	15:04:30	17	3894	3561	8
6	15:44:00	18	7486	6845	7
7	16:28:00	20	9809	8969	347
8	16:44:30	21	10,428	9535	336
9	17:19:30	22	13,803	12,621	339
10	17:25:00	23	12,734	11,644	335
11	18:02:30	24	5308	4854	285
<b>10/19/94, Clear weather</b>					
<b>Site</b>	<b>Time (local)</b>	<b>GPS Mark</b>	<b>Range (yards)</b>	<b>Range (meters)</b>	<b>Bearing<sup>1</sup> (degrees)</b>
12	9:22:30	25	4474	4091	154
13	9:47:30	26	6551	5990	163
14	10:04:00	27	7902	7226	143
15	10:28:00	28	9583	8763	125
16	10:48:00	29	10,635	9725	126
17	11:09:30	30	12,564	11,489	129
18	11:23:30	31	13,862	12,675	137
19	11:49:30	32	12,377	11,318	148
20	13:19:30	33	10,122	9256	184
21	13:45:30	34	10,571	9666	196
22	14:15:00	35	9680	8851	215
23	14:27:30	36	6935	6341	239
24	14:51:00	37	6651	6082	272
25	15:41:00	38	11,424	10,446	354
26	16:05:30	39	11,963	10,939	360
27	16:19:00	40	6397	5849	20

<sup>1</sup> Bearing from south antenna, degrees true

The method for determining effective height involves measurement of the magnetic field radiated from the antenna. Magnetic field is used instead of electric field because it is not disturbed as much by trees, buildings, etc. The formula for the magnetic field radiated by an electrically short monopole is given below, using MKS units:

$$H = \frac{Ih_e}{\lambda r} \left\{ 1 + \left( \frac{\lambda}{2\pi r} \right)^2 \right\}$$

where I = antenna current  
 $h_e$  = monopole effective height  
 r = distance from antenna  
 $\lambda$  = free space wavelength

The magnetic field is measured at many locations while accurately monitoring antenna current. The distance from the antenna to each location is also determined. The values measured are substituted into the above formula to determine the antenna effective height for each measurement. Since the antenna current can vary with time, it must be measured and recorded in real time in order to reduce the data. The distance to each measurement position must also be known. Errors in position translate directly into errors in  $h_e$ .

### 3.3.1 Antenna Current Measurements

A current monitor was installed in the helix house using a Pearson 110A current transformer and a Hewlett-Packard (HP) digital multimeter, HP 3468. The multimeter was read automatically at 30-second intervals by an HP 71 computer and the result, including measurement time, was printed. Due to the WWVB modulation format, the meter reading would normally vary 10 dB depending upon the time of reading. To eliminate this variation, it was arranged to operate using unmodulated continuous wave (CW) during the measurement. To reduce the down time required for this measurement, a cellular telephone was used so that the field strength measurement crew could notify the transmitter operator when ready for unmodulated CW for just the duration of the measurement at each site (approximately 15 minutes).

### 3.3.2 Navigation

For this series of measurements, military GPSS receivers were used, which are excellent for the surveying accuracy required. The GPS system has a feature called selective availability (SA) that derates the navigation accuracy for civilian receivers to around  $\pm 100$  meters. The military receivers used were equipped with the appropriate code, which brings the accuracy up to about  $\pm 10$  meters. This error is compensated for by (1) averaging over several minutes at each site, and (2) measuring at distances far enough away so that a 10-meter error is not a significant percentage of the total range to the transmitting antenna.

Early in the test period, the GPS was used to obtain coordinates at the monuments that mark the center of each antenna averaging over about 1/2 hour. The GPSS coordinates (WGS 84) are shown below and compared to the coordinates given to us by NIST. The GPSS and NIST coordinates agree remarkably well with a total difference of 205 feet for the north antenna and 176 feet for the south antenna. Most of this error is in the east–west coordinate, with GPSS indicating both antennas west of the NIST coordinates.

<b>GPSS (WGS 84)</b>	<b>NIST</b>
North Antenna	North Antenna
40° 40.857' north	40° 40.855' north
105° 03.034' west	105° 03.000' west
South Antenna	South Antenna
40° 40.475' north	40° 40.472' north
105° 02.688' west	105° 02.659' west

### **3.3.3 Magnetic Field Measurement**

**3.3.3.1 System Description.** The magnetic fields are measured by using a shielded loop antenna in conjunction with a tuned RF voltmeter. For the WWVB measurements, the antenna used is an approximately 1-foot by 18-inch elliptically shaped loop antenna made by Watt Engineering, potted in a blue weatherproofing compound, referred to herein as the “blue loop.” The tuned RF meter was a Hewlett-Packard selective-level meter, HP 3586. These meters specify an accuracy over a very wide band of  $\pm 0.25$  dB. We have found that in the VLF and LF band, these meters usually read the same or within 0.01 dB when compared to each other or to an HP 3446 (0.5% @ VLF and 1% @ LF).

**3.3.3.2 Calibration.** The field strength measurement system was calibrated before and after the trip to Fort Collins using the special VLF field strength calibration facility that NRaD maintains. The system uses a special 1-meter Helmholtz coil built by Watt Engineering. The Helmholtz coil calibration facility and the 60-kHz calibration data for the blue loop field strength measurement system are described in appendix D.

**3.3.3.3 Land-Based Measurements.** For land-based measurements, the HP 3586 is carried in an automobile. It is powered by an inverter connected to the car battery. The technique involves first finding a suitable area for measurements. The criteria for sites are as follows:

1. Must be accessible by automobile.
2. Must not be too close or too far away from the antenna. Much closer than a few tower heights, the above formula is not accurate enough. Farther away than 30 km or so, ionospheric effects start to impact the measurements.
3. Must be a fairly flat area. Rough terrain gives variable readings. The readings usually are high on the top of hills and low in valleys. Readings at or near discontinuities like cliffs or the seashore are often anomalous, especially if the discontinuity is in a radial direction from the transmitting antenna.
4. Must be free from metallic objects. Large steel objects perturb the magnetic fields. Sometimes, nearby fences, buried power lines or pipes, or metal buildings can give anomalous readings. If possible, buildings, fences, and power lines are kept at a distance of at least 300 meters.

In developed areas of the world, it is often difficult to find ideal sites. Often measurements are taken in the middle of parks, athletic fields, or farming fields, and sometimes on roads with no visible evidence of elevated or buried lines. Most of the area around the Fort Collins site is flat farm land, and normally it would be relatively easy to find acceptable sites. In fact, station personnel had selected many acceptable sites prior to our arrival. Unfortunately, inclement weather on the days

available for field strength measurements made access to most of the preselected sites difficult or impossible, even with four-wheel drive, due to the slippery nature of the soft clay ubiquitous to the area. Consequently, we were forced to accept some sites that were on county roads and/or not as far from fences and/or terrain variations as we would have liked.

On the first day of field strength measurements, it was raining and snowing and we were using a two-wheel drive rental van that severely limited access to sites. On the second day, we used the station's four-wheel drive truck which, combined with fine weather, afforded us better access, although the roads and fields were still wet, limiting site selection somewhat. The standard deviation of the WWVB field strength measurements is a little greater than normally experienced and is attributed to the less-than-perfect measurement sites available to us at that time. Even so, enough measurements were taken to adequately average the site variability, providing a value of effective height with acceptable accuracy for engineering purposes.

Following site selection, the vehicle was positioned and the loop is set up on the tripod about 20 feet away from the vehicle. The loop position was measured by using the GPSS receiver held near the loop antenna. We averaged these readings over several minutes. The transmitting station was called using the cellular phone and the change made to transmit in CW mode. The loop antenna was rotated for a null (minimum) reading on the tuned voltmeter and then rotated 90 degrees. Then three readings were recorded from the tuned voltmeter, synchronized by wristwatch to the measurements being taken by the HP 71 current monitor. At most locations, the loop antenna was repositioned to two other places 10 to 20 feet apart and this process repeated. Upon completion of the measurements at each site, the station was notified and normal modulation resumed.

### **3.4 MEASUREMENT RESULTS**

Measurements were made at the 27 sites identified in table 7, with (almost always) three locations at each site and three measurements per location. Figure 13 shows the results of all the measurements plotted vs. range. The average effective height is 85.5 meters. The overall sample standard deviation was 3.81 meters, which is 4.46 percent. This standard deviation is slightly greater than the 3 percent normally experienced for land-based measurements and is attributed to the reduced availability of good sites caused by inclement weather.

The deviation from the average at each site was normalized to the sample standard deviation, and measurements outside of three standard deviations were discarded as being anomalous. In this case, the measurements at site 21 were the only ones discarded. This site is in the middle of an industrial park on the north side of Fort Collins. This leaves measurements from 26 sites to be included. The standard deviation of the mean is equal to the sample standard deviation divided by the square root of the number of samples. Twice this value provides a confidence level of 99 percent. For the WWVB measurements, this amounts to  $\pm 1.49$  meters for the 99-percent error bound, which is an accuracy of within 1.75 percent.

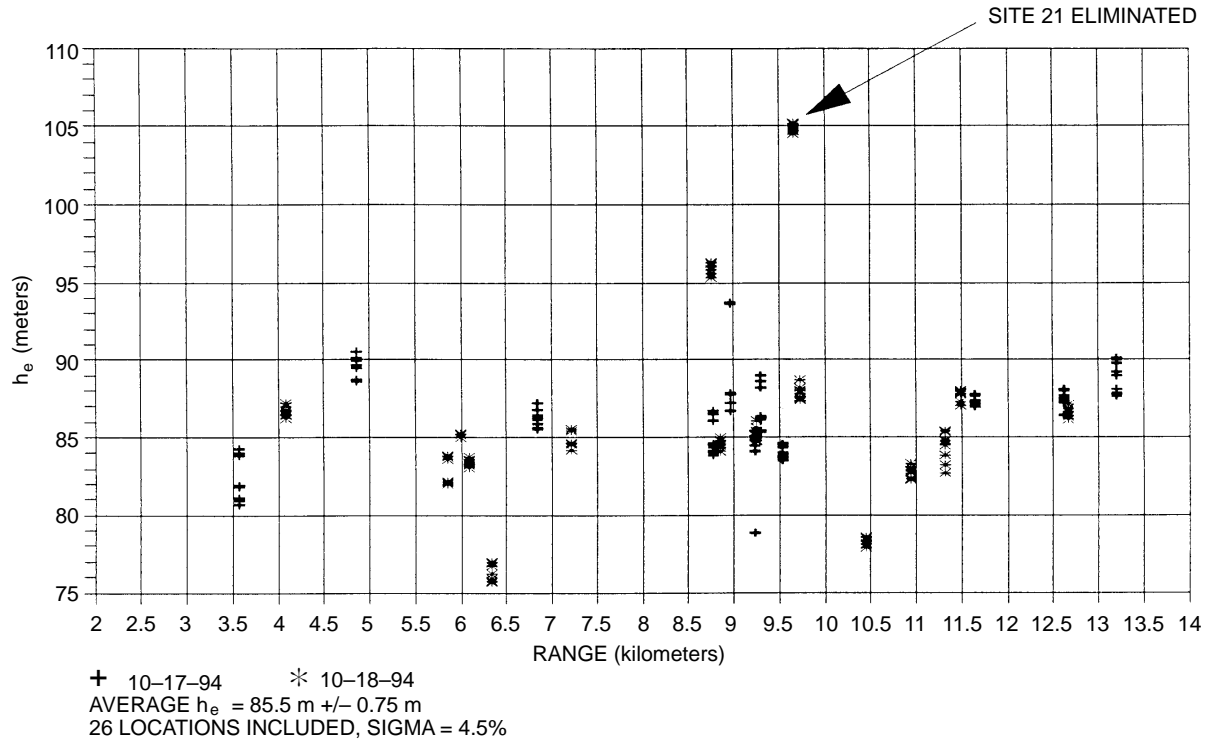


**Figure 13.** WWVB antenna effective height.

### 3.5 DISCUSSION

Radiation resistance,  $R_r$ , is calculated from  $h_e$  by the following formula:

$$R_r = 160 \left( \frac{h_e}{\lambda} \right)^2$$

where  $\lambda$  is the free space wavelength. Using the above value for effective height, the radiation resistance at 60 kHz is 0.462 ohm. Antenna and ground loss resistance is the difference between the total system resistance,  $R_g$ , and the radiation resistance, and is 0.206 ohm for the primary antenna and 0.321 ohm for the secondary antenna.

The measurements described in this report are all referred to the current measured on the low-voltage side of the helix, which is where the antenna current is monitored. Thus, radiated power is given by antenna current squared times the radiation resistance.

Radiation efficiency is given by the ratio of the radiation resistance to the total resistance. The total resistance at 60 kHz for both antennas was measured (see section 2) and is included in table 8 along with the radiation efficiency for both antennas (assuming the same  $h_e$  for both antennas).

**Table 8.** WWVB radiation efficiency (60-kHz operation).

	<b>South</b>	<b>North</b>
Effective Height, $h_e$	85.5 meters	85.5 meters
Radiation Resistance, $R_r$	0.462 ohm	0.462 ohm
Total Resistance, $R_g$	0.803 ohm	0.913 ohm
Radiation Efficiency, $\eta$	57.5%	50.6%

## 4. OTHER MEASUREMENTS

### 4.1 GENERAL

Measurements of the physical dimensions were taken of the helix house and other components, variometer, helix, bushing, insulators, wires, transmission lines, ground system, etc. These measurements are useful for estimation of various important antenna parameters such as power-handling capability, etc. Some of these data are summarized below and most are included in appendix B. A summary of the ground radial survey is included in this section.

### 4.2 LITZ WIRE

A nominal 3/4-inch-diameter litz wire is used for the helix and variometer in both helix houses. This litz wire consists of a 0.750-diameter layer of cotton lasting followed by a 0.710-diameter thin plastic coating, followed by nine bundles of insulated copper magnet wire covered by a thin cotton lasting. The bundles consist of five bundles containing five strands with 27 insulated magnet wires 0.0053 inch in diameter. The center of the wire is filled with cotton-wrapped hemp 0.320 inch in diameter. The overall specification would be  $9 \times 5 \times 5 \times 27$  #36 wires. This totals 6075 strands of #36 wire, which totals 151,875 circular mils of copper. A conservative current rating at VLF for this wire based on 1000 circular mils per amp would be 150 amps.

However, at 60 kHz the frequency effects are significant and a different method of rating is necessary. Using the technique given in Hansen (1983), based on a power dissipation limit of 1/4 watt per square inch surface area, a more realistic estimate of the current rating for the wire has been calculated as follows.

The resistance of litz wire is a function of frequency as follows:

$$R_{ac} = R_{DC} \left( 1 + \frac{f}{f_b} \right)$$

where  $f_b$  is the breakpoint frequency defined as the frequency where the AC resistance is twice the DC resistance.

Using the formulas in Hansen (1983), the breakpoint frequency for the WWVB litz is 60,039 Hz. This frequency has to be reduced to account for the effect of winding in a coil. The reference contains a graph of the breakpoint frequency reduction factor as a function of coil aspect ratio and wire spacing to diameter ratio. The WWVB helices have a wire spacing to diameter ratio,  $S/d_0 = 3$ , and a helix length to diameter ratio,  $L/D = 1$ . For these parameters, the solenoidal coil frequency reduction factor is 0.8. This gives an overall breakpoint frequency of 48 kHz for the WWVB helices. This means that the litz is being operated above the breakpoint frequency, and the AC resistance is more than twice the DC resistance (e.g.,  $R_{ac}/R_{dc} = \{1+(f/f_b)^2\} = 2.56$ ).

The current limit based on the heat dissipation for operation on frequencies at or below the breakpoint is given below.

$$I_{max} = 600 d (nd_0)^{1/2}$$

where  $d_0$  is the individual strand diameter, and  $d$  is the overall diameter of the copper.

Substitution of the values for the WWVB litz gives a maximum operating current of 209 amps. Since this litz is being operated above the operating frequency, the current must be reduced by the

square of the increase in resistance over that at the breakpoint frequency, or  $(2.56/2)^2$ , which gives a current limit of 127 amps. A conservative realistic current rating for the litz wire is thus 100 amps per strand. The south helix has three strands in parallel, which gives an estimated rating of over 300 amps; the north helix has only two strands in parallel, for an estimated rating of 200 amps.

The connectors used on the litz wire at WWVB are not the standard type that break out each individual bundle of wires. It is very likely that these connectors will be the hottest part of the system for high-current operation. As a minimum, these connectors should be replaced prior to operation with high currents.

Physical inspection indicated that the litz looks good and probably will operate at the current levels cited above. However, the litz wire itself is quite old; if the insulation on the individual strands has deteriorated, it may overheat locally when operated at high currents. If this litz is retained, it must be brought up to power slowly, undergoing a heat run to be sure it will handle the full current. Once this type of wire overheats, the insulation on the individual strands breaks down, causing further increase in resistance and heating that eventually destroys the effectiveness of the litz wire.

### 4.3 GROUND SYSTEM

The ground systems for each antenna appear to be identical and consist of approximately 300 wires, approximately 1300 feet long, buried 8 to 10 inches deep, radial to the helix house. Several of these wires were traced in the south helix house ground system by using a ground wire tracker. The results of these measurements are included in appendix B. The wires were dug up at a few locations and found to be buried at a depth of 8 to 10 inches. The buried wires are a tinned copper braid, described below, which has become somewhat brittle over the years but appears to be in generally good condition. Eventually these wires will need to be replaced, but it is not necessary at this time.

As the ground system deteriorates, the resistance increases, which decreases radiation efficiency. An excellent method of monitoring ground system condition is to keep records of antenna resistance. An analysis can then be made to determine when it is cost effective to repair or replace the ground system. When resistance increases enough to affect the power bill significantly, it is replaced. Antenna system resistance can be measured without disturbing operations by using the transmitted signal. The Navy uses a computer-based resistance monitoring system called Antenna Monitoring System (AMOS) at some LF sites. Increased antenna resistance can also be an early symptom of insulator problems.

The buried ground radials are brought back to a buried peripheral ground bus consisting of 1/2-inch copper cable running around the outside of the helix house foundation. The peripheral bus is connected to copper straps entering the cement foundation at approximately 6-foot intervals. These copper straps are presumably connected to three copper straps coming out of the cement floor inside the helix house that connect to the low side of the tuning helix. No drawings of this portion of the ground system or these hidden connections are available.

The wire used in the antenna ground systems is a tinned, stranded copper wire having an overall diameter of 0.135 inch, composed of seven strands containing 37 #34 wires (individual wire diameter 0.0065 inch). The total number of individual wires is 259, with a total area of 39.75 circular mills.

The station personnel indicated that some time ago the original ground system was examined, and the original wires had deteriorated significantly due to corrosion thought to be due to the high level of alkalinity in the soil. At that time, the ground system was upgraded, and it was decided to use the

tinned wires as a protection against corrosion; this solution seems to be working well. No drawings or documentation of the ground system upgrade are available. However, some old photographs indicate that the original ground system was a rectangular grid with large spacing between wires. The photographs also indicate that the upgraded ground systems have approximately 300 radial wires.

#### **4.4 NEAR-FIELD MEASUREMENTS UNDER TOPLOAD**

These measurements were deleted in favor of making mutual impedance measurements, which had not been scheduled. The near-field measurements would be of help in determining the locations of excessive ground losses. However, after measuring the total resistance of the antennas, it was determined that these losses were not excessive. It was decided to pursue the mutual impedance measurements instead, which are necessary to calculate the expected radiation efficiency when operating both antennas as a two-element array. If it becomes necessary, the near fields can be calculated later using an EM computer program such as NEC-IV.

## 5. REFERENCES

- Beehler, Roger E. and Michael A. Lombardi. 1991. "NIST Time and Frequency Services," NIST Special Publication 432 (June) (Revised 1990). National Institute of Standards and Technology, Boulder, CO.
- Hansen, Peder. 1983. "VLF Cutler Antenna Measurements Report," Appendix A: Litz Cable Losses, NOSC TN 1245 (January). Naval Ocean Systems Center, San Diego, CA.\*
- Sunde, Erling D. 1949. *Earth Conduction Effects In Transmission Systems*, Van Nostrand, Inc.
- Wait, James R. and Alyce M. Wahler. 1956. "On the Measurement of Ground Conductivity at VLF," NBS Report 5037 (December). National Bureau of Standards.

---

\* NRaD Technical Notes (TNs) are working documents and do not represent an official policy of the NCCOSC RDT&E Division. For further information, contact the author.



**APPENDIX A:**  
**RAW BASELINE IMPEDANCE DATA**

## A.1 Data Disk

The antenna and tuning system characterizations were performed using a network analyzer and a specialized impedance probing technique tailored for the large structures associated with VLF or LF antennas and antenna tuning equipment. The recorded measurements were complex impedance measurements (magnitude and phase) of the antenna and antenna tuning components.

All of the raw data gathered by the network analyzer and used to prepare this report have been stored on a 3½-inch floppy disk. The network analyzer is the Hewlett-Packard Model HP 4195A. The characteristics of the analyzer require that a separate instrument status file is loaded into the instrument prior to the recall of the data in order to display the data correctly. The data recorded on the disk is catalogued and described in table A-1. The instrument state to be used with each data file is shown in the table. The data disk is not included in this report, but is available upon request from the NRaD task coordinator.

**Table A-1.** WWVB data disk log. Page 1 of 2

State File	Data File	Descriptive Title	Comments
W1S	W1D	Primary Antenna System $R_{gross}$ and Bandwidth, 2 kHz Span	Secondary antenna grounded
W2S	W2D	Primary Antenna System $R_{gross}$ and Bandwidth, 1 kHz Span	Secondary antenna grounded
W3S	W3D	Primary Antenna System $R_{gross}$ and Bandwidth, 2 kHz Span	Secondary antenna floating (1 M $\Omega$ static drain)
W4S	W4D	Primary Antenna System Resistance with Parasitic Secondary at 60 kHz	XMSN line disconnected, Real and Imaginary
W5S	W5D	Primary Antenna System Resistance with Parasitic Secondary at 60 kHz	XMSN line disconnected, Magnitude and Phase
W6S	W6D	Primary Antenna Impedance, 10 kHz to 1 MHz	Secondary antenna grounded
W7S	W7D	Primary Antenna Impedance, 20 kHz to 100 kHz	Secondary antenna grounded
W8S	W8D	Primary Antenna Impedance, 4 kHz to 400 kHz	Secondary antenna grounded
W9S	W9D	Secondary Antenna System Resistance with Parasitic Primary at 60 kHz	XMSN line disconnected, Real and Imaginary
W10S	W10D	Secondary Antenna System $R_{gross}$ at 60 kHz, 1 kHz Span	XMSN line disconnected, Wet insulators!
W11S	W11D	Secondary Antenna Impedance, 10 kHz to 1 MHz	Primary antenna grounded
W12S	W12D	Secondary Antenna Impedance, 4 kHz to 400 kHz	Primary antenna grounded
W13S	W13D	Helix Primary Impedance, Secondary Helix House, 10 kHz Span	Primary antenna grounded
W14S	W14D	Helix Primary Impedance, Secondary Helix House, 1 kHz Span	Primary antenna grounded
W15S	W15D	Helix Primary Impedance, Secondary Helix House, with 27 nF Capacitors	Primary antenna grounded
W16S	W16D	Secondary Antenna System $R_{gross}$ and Bandwidth	After running XMTR for 2 hours to dry insulators
W17S	W17D	Helix Primary Impedance, Secondary Helix House, 10 kHz Span	After running XMTR for 2 hours to dry insulators
W18S	W18D	Helix Primary Impedance, Secondary Helix House, 1 kHz Span	After running XMTR for 2 hours to dry insulators
W19S	W19D	Helix Primary Impedance, Secondary Helix House, with Capacitors	27 nF capacitor in series with each leg
W20S	W20D	Primary Antenna System $R_{gross}$ and Bandwidth, 1 kHz Span	After running XMTR for 2 hours to dry insulators

**Table A-1.** WWVB data disk log. Page 2 of 2

<b>State File</b>	<b>Data File</b>	<b>Descriptive Title</b>	<b>Comments</b>
W21S	W21D	Helix "Blue" Primary Impedance, Primary Helix House, 5 kHz Span	No Capacitors
W22S	W22D	Helix "Blue" Primary Impedance, Primary Helix House, 1 kHz Span	No Capacitors
W23S	W23D	Helix "Grey" Primary Impedance, Primary Helix House, 5 kHz Span	No Capacitors
W24S	W24D	Helix "Grey" Primary Impedance, Primary Helix House, 1 kHz Span	No Capacitors
W25S	W25D	Helix "Blue" Primary Impedance, Primary Helix House, with Capacitors	27 nF in series with each leg
W26S	W26D	Helix "Grey" Primary Impedance, Primary Helix House, with Capacitors	Total of 44 nF in series with one leg
W27S	W27D	Mutual Impedance of Primary Antenna with Parasitic Secondary at 60 kHz	Magnitude and Phase
W28S	W28D	Mutual Impedance of Secondary Antenna with Parasitic Primary at 60 kHz	Real and Imaginary
W29S	W29D	Mutual Impedance of Secondary Antenna with Parasitic Primary at 60 kHz	Magnitude and Phase
W30S	W30D	Secondary Antenna System Input Resistance with Primary Grounded	Used with W29 above for Mutual calculations
W31S	W31D	Primary Transmission Line Input Impedance with "Grey" Helix Primary Connected	Magnitude and Phase, with capacitors
W32S	W32D	Primary Transmission Line Input Impedance with "Grey" Helix Primary Connected	Real and Imaginary
W33S	W33D	Primary Transmission Line Input Impedance with "Grey" Helix Primary Connected	Magnitude and Phase, without capacitors
W34S	W34D	Secondary Transmission Line Input Impedance	Tuned with XMTR
W35S	W35D	Secondary Transmission Line Input Impedance, Retuned	Tuned for $Z_{max}$ at 60 kHz
W36S	W36D	Plate-To-Plate Impedance of "Grey" Transmitter with Primary Antenna	Tuned with XMTR



**APPENDIX B:**  
**PHYSICAL MEASUREMENTS**

## B.1 Transmission Line Distances

Length from transmitter building (outside wall) to helix house (outside wall).

B.1.1 WWVB North (Secondary) Helix to transmitter building: 1343'

Secondary within transmitter building: 26'

Secondary within helix: 44'

Total: 1413'

$$\% \text{ Sag} = (8 \text{ inch}) / (120 \text{ ft}) (12 \text{ inch}) \times 100\% = 0.56\%$$

B.1.2 WWVB South (primary) helix to transmitter building: 1342.5'

Primary within transmitter building: 13.0'

Primary within helix building: 40.0'

Total: 1395.5'

$$\% \text{ Sag} = (8 \text{ inch}) / (120 \text{ ft}) (12 \text{ inch}) \times 100\% = 0.56\%$$

B.1.3. Conductors:

Spacing of wires: 20"

Diameter of wires: 0.494"

Height of wires above ground: 19' 8"

Typical distance between poles: 120'

## B.2 North (Backup) Helix House

B.2.1. Exterior house dimensions:

24' height X 21' width X 32' depth

Width detail left to right – 3', 6' (doors), 12'

Front two doors: 3' X 6' 8" height (each)

(Note approx. 18' interior width)

B.2.2. Variometer Dimensions:

Pedestal: 44" high

3'6" minimum diameter

5'6" maximum diameter

2' inner diameter

Variometer: 35" width X 19" height

set on insulators 11" height each

Top 1/2 stator and bottom 1/2 stator: 4 turns of double litz.

Top 1/2 rotor and bottom 1/2 rotor: 4 turns of double litz

Rotor series connected between 1/2 stator sections

B.2.3. North Helix Dimensions:

Helix diameter is 74"

5 fingers per porcelain ring to support litz wire  
11 turns of 60 kHz secondary + 20' of litz  
4 turns of 60 kHz primary (blue transmitter)

B.2.4. Size of Corona Ring on top of helix:

Outer diameter is 80"  
Inner diameter is 74 "  
Tube diameter is 3"  
Ring separation from 3 helix walls is 69–70"  
Ring separation from helix ceiling about 102"

B.2.5. Size of pipe going through bushing:

Diameter is 4 1/2"  
Ground ball diameter about 9" with 7" gap when open

**B.3 South (Primary) Helix House**

B.3.1. Exterior House Dimensions: Same as North

B.3.2. Variometer Dimensions: Same as North

Windings: Same as North  
Connection: Rotor parallel connected across both 1/2 stator sections that are connected in series

B.3.3. South Helix Dimensions: Diameter is same as North

Height is less but not measured  
Helix diameter is 74"  
5 fingers per porcelain ring to support litz wire  
Secondary winding (60 Khz): 15 4/5 turns triple litz wire + 3' of additional litz  
Primary windings: 1 4/5 4 turns single litz (blue transmitter)  
5 5/4 turns single litz (grey transmitter)

B.3.4. Bushing and ground ball: Same as North

Spare bushing has 8 holes in top ring and 18 holes in bottom ring

B.3.5. North Helix House Roof

The roof is galvanized steel with a raised mesh catwalk around the bushing and under the pull off insulator assembly. The bushing with its aluminum mounting pedestal is on a raised platform square 4" above the roof.

Aluminum corona ring at top center of bushing assembly (same as corona ring with pull off insulator):

Ring outer diameter:	22"
Ring inner diameter:	17"
Ring tube diameter:	2.5"
Height from flange to top of ring surface:	7.5"

40", vertical, from outer flange of rain shield to feed wire	
Bushing rain shield:	
Outer diameter ring	63"
Inner diameter ring	55"
Tube diameter	4"
Overall height of shield	12"
Height from top center to roof	78"
Height from ring edge to roof	66"
Bushing:	
Minor diameter	21 1/2"
Major diameter	40 1/2"
Height	34"
Aluminum pedestal bushing sits on:	
Major diameter	54"
Minor diameter	48 1/2"
Height	32"
Ball Gap diameter:	8.9 inches
West side gap to rain shield ring	13.5"
East side gap to rain shield ring	16"
Pull off insulator and corona ring assembly:	
Insulator diameter	4"
Insulator length stud hole to stud hole:	76"
Rod length from insulator to center	30" (plan)
Corona ring dimensions the same as the corona ring at center of bushing.	
Distance from roof to Corona ring	55 1/2"

## B.4 Antenna

### B.4.1. Feed Cage:

North (Secondary) side: 5 5/8" diameter with 0.25" diameter, 6 cables each, with each cable consisting of 7 aluminum strands.

South (Primary) side: 5 5/8" diameter with 0.248" diameter wire, 6 cables each, with 7 strands, but the center strand is steel surrounded by 6 aluminum strands.

### B.4.2. Main Insulators at Towers:

Approximately 48" of smooth hollow 4 inch-diameter porcelain tubes.  
Connected two in parallel for strength

### B.4.3. Towers, leg diameter, face size (center to center), and height (from drawings)

Face size:	4'
Heights:	
Far outside West Tower on Primary antenna:	420' 0"

All other towers: 401' 6"  
Leg diameter: 2 1/2"

## **B.5 Ground Wire Survey Information at South (Primary) Helix**

### **B.5.1. Helix Location at West Side Wall (center):**

N 40° 40.484' (Mark 01)  
W 105° 02.709'

### **B.5.2. Ground Radials:**

Ground radial found and left uncovered (8" – 10" deep)

N 40° 40.445'  
W 105° 02.750'

Ground radial left uncovered (8" – 10" deep)

N 40° 40.409'  
W 105° 02.778'

Ground radial located but broken

N 40° 40.398' (Mark 02)  
W 105° 02.789'

Ground radial located:

N 40° 40.378'  
W 105° 02.797'

Ground radial located:

N 40° 40.335' (Mark 03)  
W 105° 02.836'

Distance to helix house (Mark 01) is 1065.4'

Ground radial located:

N 40° 40.305' (Mark 04)  
W 105° 02.863'

Distance to helix house (Mark 01) is 1293.2'.

Could not locate end of radial, but estimate the end is no more than 5–10 yards more.

(Numbers 4, 5, 6 are on same radial)

### **B.5.3. Radial Count of South (Primary) Helix using Ground Wire Detector:**



**APPENDIX C:**  
**WWVB ANTENNA CURRENT METER CALIBRATION**

### C.1 WWVB Antenna Current Meter Calibrations

There are antenna current monitors in both helix houses. They are quite old and appear to use a bolometer type of detector that is nonlinear. There are meters located in each helix house that read current as well as a remote meter in the transmitter building. These meters were calibrated using a Pearson current transformer and a Hewlett-Packard digital multimeter. The Pearson current monitors are calibrated in the factory and are expected to be accurate to within  $\pm 1\%$ . The transmitter was operated using unmodulated CW and set to several power levels. This was done for both the north and south helix houses. The calibration data are shown in figures C-1 and C-2, and the data are listed in table C-1 below.

**Table C-1.** Antenna current meter calibration data.

Backup Helix House Currents 10-13-94			Primary Helix House Currents 10-14-94		
Xmtr Meter	Helix House Meter	Pearson 110 (Amperes)	Xmtr Meter	Helix House Meter	Pearson 110 (Amperes)
	0	0	0	0	0
	6	48	41.5	9.03	75
25	7.5	53.3	49	11.04	85
30	15	75.5	63	16	106
31.3	17.5	81.6	68	18.6	114
32	19	84.5	75	22	124
35	22	90.8	81	23.976	132
37.5	27	99.3	84	26	137
39	29	103	88	27.5	142
39	30	104.6	91	28.5	146
45	36	115.1			
47	43	126			
* 45	47	133			
	52	139			

\* Xmtr meter sticking at the upper end of the range.

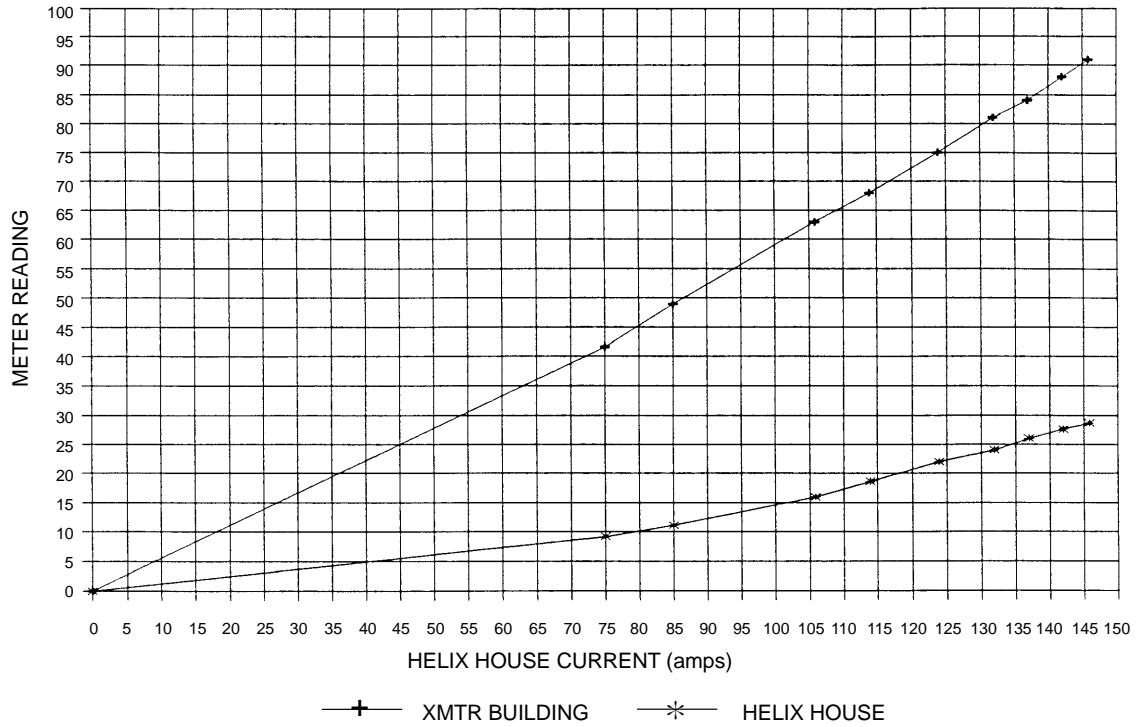
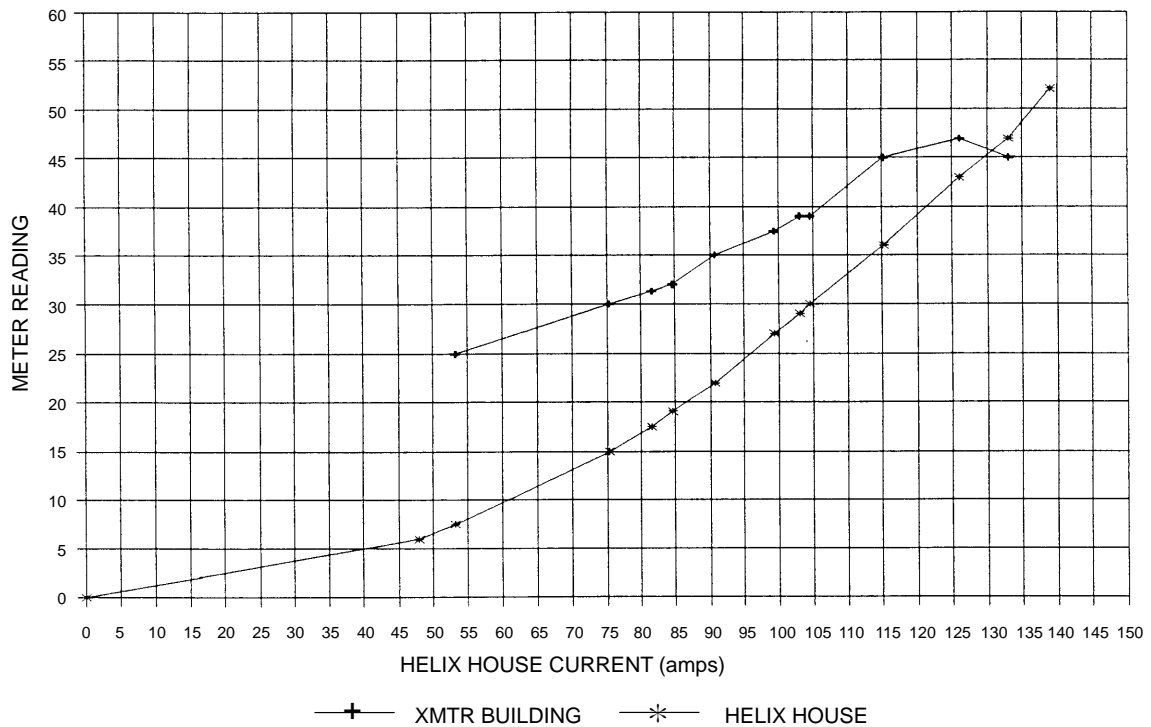


**Figure C-1.** Primary antenna current meter calibration.



NOTE: XMTR METER WAS STICKING AT THE UPPER END OF THE RANGE OF DATA.

**Figure C-2.** Secondary antenna current meter calibration.



**APPENDIX D:**  
**HELMHOLTZ COIL CALIBRATION**

## D.1 Calibration of the Field Strength Measurement System

NRaD maintains a special field strength calibration facility for the Space and Naval Warfare Systems Command (SPAWAR). The magnetic field strength calibration consists of a 1-meter Helmholtz coil constructed by Watt Engineering. The Helmholtz coil is located in a special building constructed so as not to disturb the magnetic fields of the Helmholtz coil during calibration.

The Helmholtz coil is used to generate a magnetic field of known strength. It consists of two single-turn loops having a 1-meter radius and spaced 1 meter apart. The loops are connected in series so that they carry the same current. A precision 10-ohm resistor is connected on the ground side of the input to the Helmholtz coil to provide an accurate method of measuring current. The calibration setup is shown in figure D-1. The Helmholtz coil geometry provides the maximum volume of uniform magnetic field for a two-loop system.

The field in the center of the Helmholtz coil is given by the following equation for one turn on each part of the coil.

$$H = \frac{I}{a \left(\frac{5}{4}\right)^{\left(\frac{3}{2}\right)}}$$

where  $a$  is the radius of the Helmholtz coil, which in our case is 1 meter.

The calibration of the Helmholtz coil system is checked prior to the calibration of a field strength measurement system by using a standard four-turn air core loop. The results of calibration checks before and after the trip to Fort Collins, shown in figures D-2 and D-3, indicate that a calibration accuracy of better than 0.1 dB can be expected for up to 100 kHz for this system. The increase in signal above 100 kHz is attributed to resonance of the standard antenna system including the feed coax. The actual upper frequency limit for the 1-meter Helmholtz coil system is probably on the order of 1 MHz or so.

For the air core loop calibration checks, two HP 3586 selective-level meters were used that exhibit an accuracy of better than 0.1 dB in the LF band. One is used to measure the Helmholtz coil current and the other is used to measure the voltage induced in the air core loop. A large part of the variability in figures D-2 and D-3 is attributed to the difference in response of these two meters over the frequency band. This effect can be eliminated by using the same meter to measure Helmholtz current and loop response. For this case, the calibration depends entirely upon geometry and the accuracy of the current measurement. Absolute accuracy and repeatability observed for air core loop calibrations using this technique have been better than  $\pm 0.025$  dB.

The calibration procedure consists of driving the Helmholtz coil with a synthesizer, measuring the RF current in the Helmholtz coil, and calculating the magnetic field using the above equation. The loop to be calibrated is placed in the center of the Helmholtz coil, and the output response is measured.

The calibration data for the “blue loop” at 60 kHz are shown in figures D-4 and D-5. The data are given in terms of the equivalent effective height,  $h_e'$ . Traditionally, the results of field strength measurements are given in terms of equivalent electric field ( $E'$ ) even though magnetic field is measured. The equivalent electric field is related to the magnetic field by the impedance of free space ( $120\pi$  ohms). The equivalent effective height of a field strength measurement system relates the meter reading to the equivalent electric field as follows:

$$120\pi H h_e' = E' h_e' = V_{\text{loop}}$$

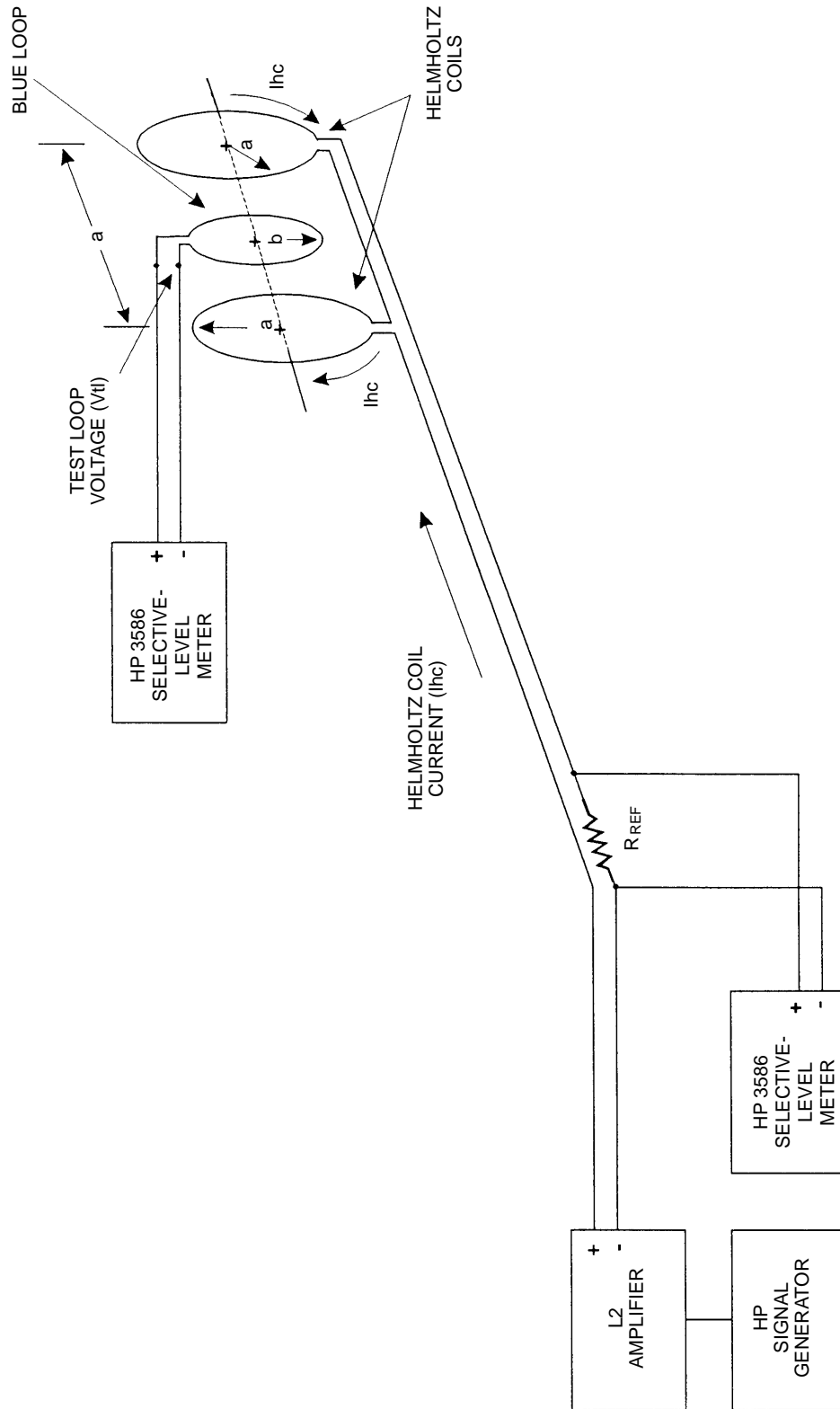


**Figure D-1.** Helmholtz coil calibration setup.

The blue loop was operated unterminated for the WWVB measurements. The equivalent effective height for the blue loop for large signals was measured to be 8.284 mm prior to leaving for Fort Collins (figure D-4) and 8.221 mm (figure D-5) on return from Fort Collins. The average of these two values, 8.253 mm, was used to process the field strength measurements to determine the transmitting effective height of the primary WWVB antenna.

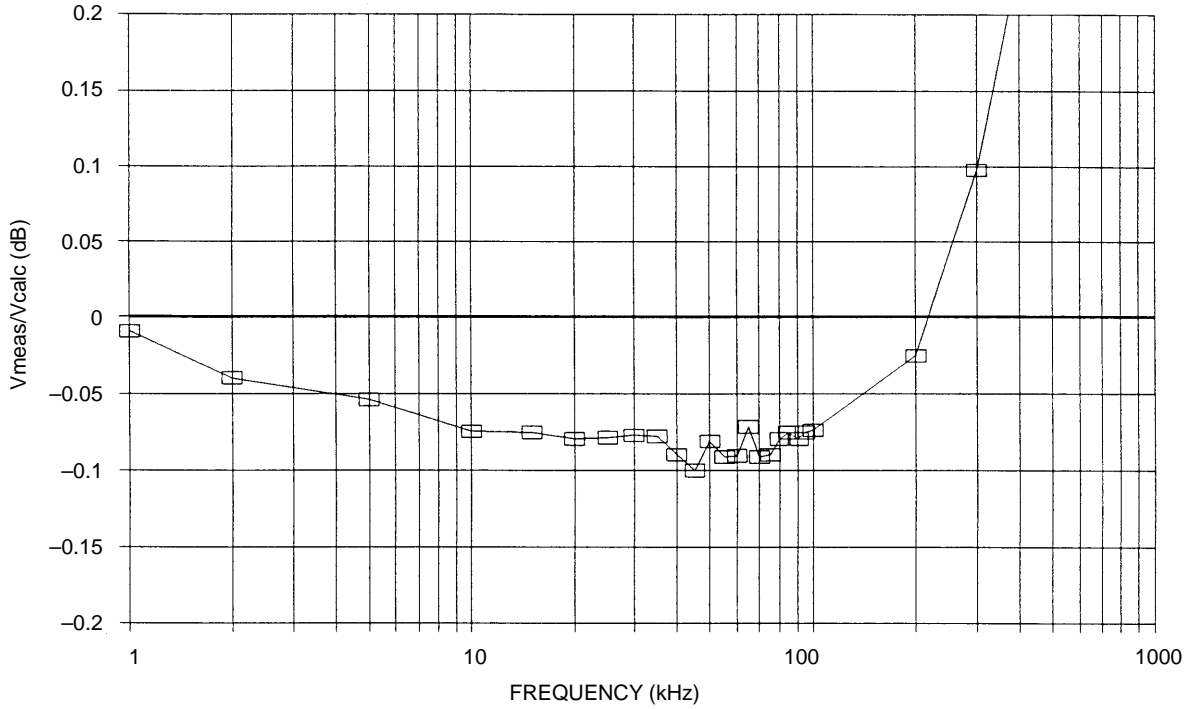


**Figure D-2.** Helmholtz coil calibration, before measurements.

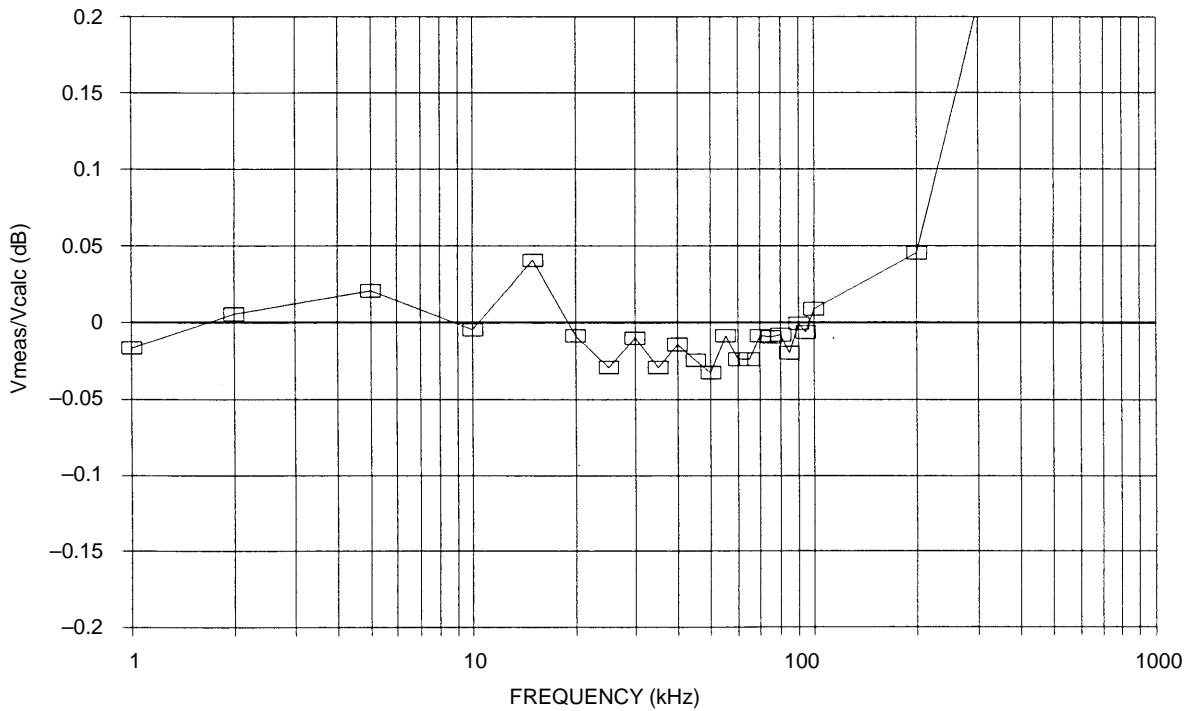


**Figure D-3.** Helmholtz coil calibration, after measurements.

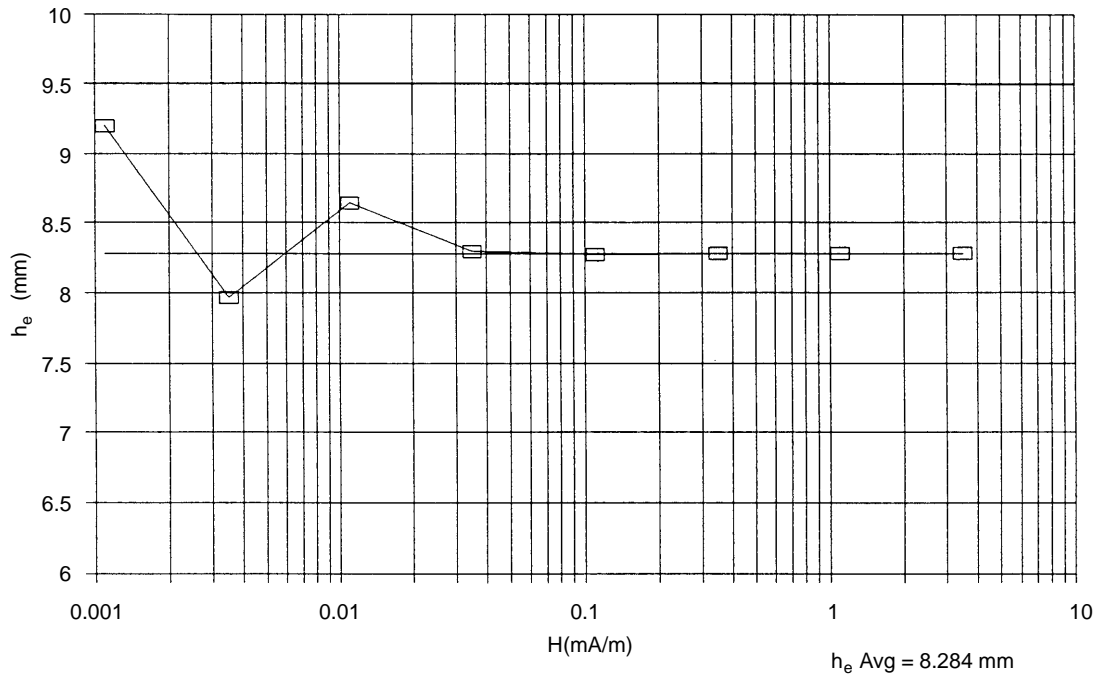


**Figure D-4.** Blue loop calibration, before measurements.

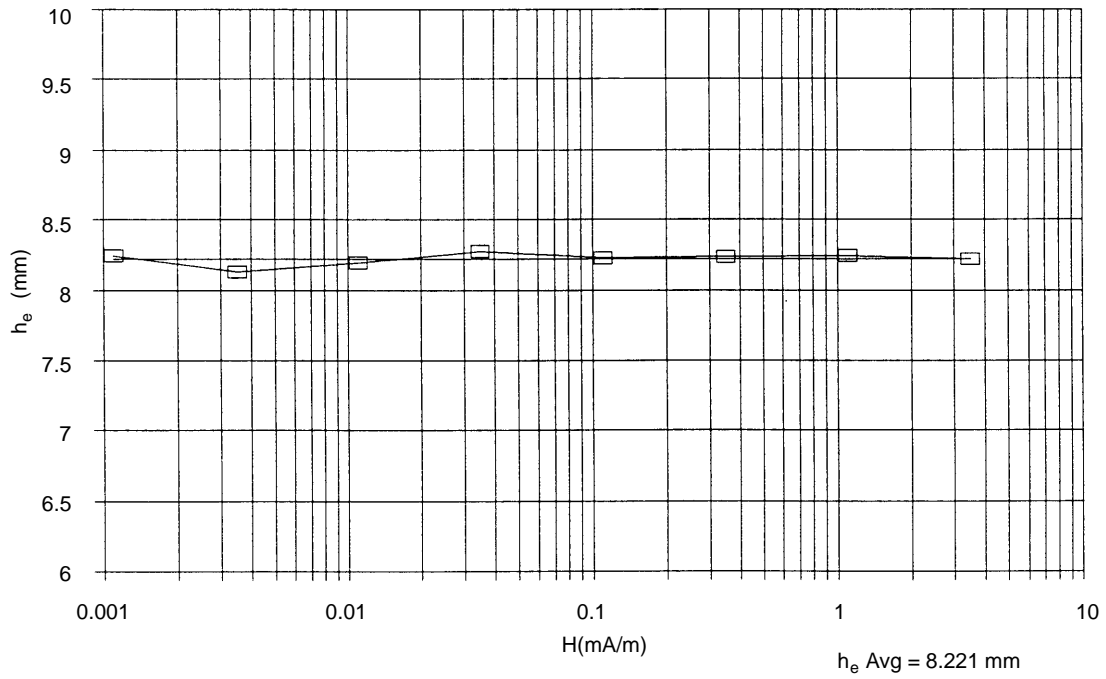


**Figure D-5.** Blue loop calibration, after measurements.



# REPORT DOCUMENTATION PAGE

*Form Approved*  
OMB No. 0704-0188

Public reporting burden for this collection of information is estimated to average 1 hour per response, including the time for reviewing instructions, searching existing data sources, gathering and maintaining the data needed, and completing and reviewing the collection of information. Send comments regarding this burden estimate or any other aspect of this collection of information, including suggestions for reducing this burden, to Washington Headquarters Services, Directorate for Information Operations and Reports, 1215 Jefferson Davis Highway, Suite 1204, Arlington, VA 22202-4302, and to the Office of Management and Budget, Paperwork Reduction Project (0704-0188), Washington, DC 20503.

1. AGENCY USE ONLY <i>(Leave blank)</i>		2. REPORT DATE <p style="text-align: center;">September 1994</p>		3. REPORT TYPE AND DATES COVERED <p style="text-align: center;">Final; Sep 1993 – Sep 1994</p>	
4. TITLE AND SUBTITLE <p style="text-align: center;"><b>CHARACTERIZATION AND SIMULATION OF AN ACOUSTIC SOURCE MOVING THROUGH AN OCEANIC WAVEGUIDE</b></p>			5. FUNDING NUMBERS <p style="text-align: center;">PE: 0602435N SUBPROJ: RJ35C72 WU: DN304159</p>		
6. AUTHOR(S) <p style="text-align: center;">Michael Reuter</p>			8. PERFORMING ORGANIZATION REPORT NUMBER <p style="text-align: center;">TR 1673</p>		
7. PERFORMING ORGANIZATION NAME(S) AND ADDRESS(ES) <p style="text-align: center;">Naval Command, Control and Ocean Surveillance Center (NCCOSC) RDT&amp;E Division San Diego, CA 92152-5001</p>					
9. SPONSORING/MONITORING AGENCY NAME(S) AND ADDRESS(ES) <p style="text-align: center;">Office of Chief of Naval Research Arlington, VA 22217-5000</p>			10. SPONSORING/MONITORING AGENCY REPORT NUMBER		
11. SUPPLEMENTARY NOTES					
12a. DISTRIBUTION/AVAILABILITY STATEMENT <p style="text-align: center;">Approved for public release; distribution is unlimited.</p>				12b. DISTRIBUTION CODE	
13. ABSTRACT <i>(Maximum 200 words)</i>  <p style="text-align: center;">This report presents a time-varying linear-systems interpretation of the moving-acoustic-source problem. We present an algorithm that simulates the time series received at a sensor or an array of sensors resulting from the moving source. We then compare simulated data to experimental data to demonstrate the potential of the algorithm.</p>					
14. SUBJECT TERMS <p style="text-align: center;">broadband modeling moving acoustic source nonstationary processes time series simulation underwater acoustics</p>				15. NUMBER OF PAGES	
17. SECURITY CLASSIFICATION OF REPORT <p style="text-align: center;">UNCLASSIFIED</p>				16. PRICE CODE	
				20. LIMITATION OF ABSTRACT <p style="text-align: center;">SAME AS REPORT</p>	
18. SECURITY CLASSIFICATION OF THIS PAGE <p style="text-align: center;">UNCLASSIFIED</p>		19. SECURITY CLASSIFICATION OF ABSTRACT <p style="text-align: center;">UNCLASSIFIED</p>		20. LIMITATION OF ABSTRACT <p style="text-align: center;">SAME AS REPORT</p>	

UNCLASSIFIED

21a. NAME OF RESPONSIBLE INDIVIDUAL Michael Reuter	21b. TELEPHONE <i>(include Area Code)</i> (619) 553-2045	21c. OFFICE SYMBOL Code 712